12-239

REACTOR VESSEL MATERIAL SURVEILLANCE PROGRAM FOR INDIAN POINT UNIT NO. 2 ANALYSIS OF CAPSULE T

by

E. B. Norris

FINAL REPORT

SwRI Project 02-4531

to

Consolidated Edison Company of New York, Inc.

4 Irving Place

New York, New York 10003

June 30, 1977

SOUTHWEST RESEARCH INSTITUTE

SAN ANTONIO CORPUS CHRISTI HOUSTON

ERRATA SHEET (Dec., 1978)

"Reactor Vessel Material Surveillance
Program for Indian Point Unit No. 2
Analysis of Capsule T" (June 30, 1977)

(1) pg. 18, TABLE III: The Measured activities of Cu, Ni and Co given in Column 3 are one order of magnitude too high (e.g., 5.28×10^{2} for Cu should be 5.28×10^{1}, etc.).

(2) pg. 30, TABLE IX: The C_V Upper Shelf Energy (ft-lb) for the Correlation Monitor[4] should be:

Unirradiated:	78
Irradiated:	68
E, ft-lbs:	10
E, %	13

(3) pg 42, paragraph(3):

$105^{\circ}F$	should be	$110^{\circ}F$
$270^{\circ}F$	should be	$280^{\circ}F$
$130^{\circ}F$	should be	$140^{\circ}F$

SOUTHWEST RESEARCH INSTITUTE
Post Office Drawer 28510, 8500 Culebra Road
San Antonio, Texas 78284

REACTOR VESSEL MATERIAL SURVEILLANCE PROGRAM FOR INDIAN POINT UNIT NO. 2 ANALYSIS OF CAPSULE T

by
E. B. Norris

FINAL REPORT
SwRI Project 02-4531

to
Consolidated Edison Company of New York, Inc.
4 Irving Place
New York, New York 10003

June 30, 1977

Approved:

U. S. Lindholm, Director
Department of Materials Sciences

P

ABSTRACT

The first vessel material surveillance capsule removed from the Indian Point Unit No. 2 nuclear power plant has been tested, and the results have been evaluated. Heatup and cooldown limit curves for normal operation have been developed for up to 5 effective full power years of operation.

TABLE OF CONTENTS

		Page
LIST OF TABLES		iv
LIST OF FIGURES		v
I.	SUMMARY OF RESULTS AND CONCLUSIONS	1
II.	BACKGROUND	3
III.	DESCRIPTION OF MATERIAL SURVEILLANCE PROGRAM	7
IV.	TESTING OF SPECIMENS FROM CAPSULE T	13
V.	ANALYSIS OF RESULTS	34
VI.	HEATUP AND COOLDOWN LIMIT CURVES FOR NORMAL OPERATION OF INDIAN POINT UNIT NO. 2	42
VII.	REFERENCES	49
APPENDIX A - TENSILE TEST RECORDS		
APPENDIX B - PROCEDURE FOR THE GENERATION OF ALLOWABLE PRESSURE-TEMPERATURE LIMIT CURVES FOR NUCLEAR POWER PLANT REACTOR VESSELS		

LIST OF TABLES

Table		Page
I	Indian Point Unit No. 2 Reactor Vessel Surveillance Materials	9
II	Summary of Reactor Operations Indian Point Unit No. 2	16
III	Summary of Neutron Dosimetry Results Capsule T	18
IV	Fast Neutron Spectrum and Iron Activation Cross Sections for Capsule T	20
V	Charpy V-Notch Impact Data Indian Point Unit No. 2 Pressure Vessel Shell Plate B2002-1	22
VI	Charpy V-Notch Impact Data Indian Point Unit No. 2 Pressure Vessel Shell Plate B2002-2	23
VII	Charpy V-Notch Impact Data Indian Point Unit No. 2 Pressure Vessel Shell Plate B2002-3	24
VIII	Charpy V-Notch Impact Data Correlation Monitor Material (Supplied by U. S. Steel)	25
IX	Notch Toughness Properties of Capsule T Specimens Indian Point Unit No. 2	30
X	Tensile Properties of Surveillance Materials Capsule T	31
XI	Projected Shifts in RT_{NDT} for Indian Point Unit No. 2	39
XII	Proposed Reactor Vessel Surveillance Capsule Schedule Indian Point Unit No. 2	41

LIST OF FIGURES

Figure		Page
1	Arrangement of Surveillance Capsules in the Pressure Vessel	8
2	Vessel Material Surveillance Specimens	11
3	Arrangement of Specimens and Dosimeters in Capsule T	12
4	Effect of Irradiation on C_V Impact Properties of Indian Point Unit No. 2 Shell Plate B2002-1	26
5	Effect of Irradiation on C_V Impact Properties of Indian Point Unit No. 2 Shell Plate B2002-2	27
6	Effect of Irradiation on C_V Impact Properties of Indian Point Unit No. 2 Shell Plate B2002-3	28
7	Effect of Irradiation on C_V Impact Properties of Indian Point Unit No. 2 Correlation Monitor Material	29
8	Dependence of C_V Shelf Energy on Neutron Fluence, Indian Point Unit No. 2	36
9	Effect of Neutron Fluence on RT_{NDT} Shift, Indian Point Unit No. 2	38
10	Estimated Transverse Charpy V-Notch Properties of Plate B2002-3	44
11	Indian Point Unit No. 2 Reactor Coolant Heatup Limitations Applicable for Periods up to 5 Effective Full Power Years	46
12	Indian Point Unit No. 2 Reactor Coolant Cooldown Limitations Applicable for Periods up to 5 Effective Full Power Years	47
13	Indian Point Unit No. 2 Inservice Leak Test Limitations Applicable for Periods up to 5 Effective Full Power Years	48

I. SUMMARY OF RESULTS AND CONCLUSIONS

The analysis of the first material surveillance capsule removed from the Indian Point Unit 2 reactor pressure vessel led to the following conclusions:

(1) Based on a calculated neutron spectral distribution, Capsule T received a fast fluence of 2.02×10^{18} neutrons/cm^2 > 1 MeV.

(2) The surveillance specimens of the three core beltline plates experienced shifts in transition temperature of 85°F to 130°F as a result of the above exposure.

(3) Plate B2002-3 exhibited the largest shift and will control the heatup and cooldown limitations.

(4) The estimated maximum neutron fluence of 6.97×10^{17} neutrons/cm^2 > 1 MeV received by the vessel wall accrued in 1.42 full power years. Therefore, the projected maximum neutron fluence after 32 effective full power years (EFPY) is 1.57×10^{19} neutrons/cm^2 > 1 MeV. This estimate is based on a lead factor of 2.9 between Capsule T and the point of maximum pressure vessel flux.

(5) Based on Regulatory Guide 1.99 trend curves, the projected maximum shift in ductile-brittle transition temperature of the Indian Point Unit 2 vessel core beltline plates at the 1/4T and 3/4T positions after 5 EFPY of operation are 110°F and 50°F, respectively. These values were used as the bases for computing heatup and cooldown limit curves for up to 5 EFPY of operation.

(6) The maximum shifts in the transition temperature of the Indian Point Unit 2 vessel core beltline plates at the 1/4T and 3/4T positions after 32 EFPY of operation are projected to be 280 °F and 140 °F, respectively.

(7) The Indian Point Unit 2 vessel plates located in the core beltline region are projected to retain sufficient toughness at the 1/4T and 3/4T positions to meet the current requirements of 10CFR50 Appendix G throughout the design life of the unit.

II. BACKGROUND

The allowable loadings on nuclear pressure vessels are determined by applying the rules in Appendix G, "Fracture Toughness Requirements," of 10CFR50.[1]* In the case of pressure-retaining components made of ferritic materials, the allowable loadings depend on the reference stress intensity factor (K_{IR}) curve indexed to the reference nil ductility temperature (RT_{NDT}) presented in Appendix G, "Protection Against Non-ductile Failure," of Section III of the ASME Code.[2] Further, the materials in the beltline region of the reactor vessel must be monitored for radiation-induced changes in RT_{NDT} per the requirements of Appendix H, "Reactor Vessel Material Surveillance Program Requirements," of 10CFR50.

The RT_{NDT} is defined in paragraph NB-2331 of Section III of the ASME Code as the highest of the following temperatures:

(1) Drop-weight Nil Ductility Temperature (DW-NDT) per ASTM E208;[3]

(2) 60 deg F below the 50 ft-lb Charpy V-notch (C_V) temperature;

(3) 60 deg F below the 35 mil C_V temperature.

The RT_{NDT} must be established for all materials, including weld metal and heat affected zone (HAZ) material as well as base plates and forgings, which comprise the reactor coolant pressure boundary.

It is well established that ferritic materials undergo an increase in strength and hardness and a decrease in ductility and toughness when exposed

---

* Superscript numbers refer to references at the end of the text.

to neutron fluences in excess of 10^{17} neutrons per cm^2 ($E > 1$ MeV).[4] Also, it has been established that tramp elements, particularly copper and phosphorous, affect the radiation embrittlement response of ferritic materials.[5-7] The relationship between increase in RT_{NDT} and copper content is not defined completely. For example, Regulatory Guide 1.99, originally issued in July 1975, and revised in April 1977[7], proposes an adjustment to RT_{NDT} proportional to the square root of the neutron fluence. Westinghouse Electric Corporation, in their comments on the 1975 issue of Regulatory Guide 1.99[8], believed that the proposed relationship overestimates the shift at fluences greater than 1.9×10^{19} and underestimates the shift at fluences less than 1.9×10^{19}. On the other hand, Combustion Engineering, in their comments on the 1975 issue of Regulatory Guide 1.99[9], suggested that the proposed relationship is overly conservative at fluences below 10^{19} neutrons per cm^2 ($E > 1$ MeV). There is also disagreement concerning the prediction of C_v upper shelf response to exposure to neutron irradiation.[7-9] After reviewing the comments and evaluating additional surveillance program data, the NRC issued a revision to Regulatory Guide 1.99 which raised the upper limit of the transition temperature adjustment curve. In this report, estimates of shifts in RT_{NDT} are based on Regulatory Guide 1.99, Revision 1.[7]

In general, the only ferritic pressure boundary materials in a nuclear plant which are expected to receive a fluence sufficient to affect RT_{NDT} are those materials which are located in the core beltline region of the reactor

pressure vessel. Therefore, material surveillance programs include specimens machined from the plate or forging material and weldments which are located in such a region of high neutron flux density. ASTM E 185[10] describes the current recommended practice for monitoring and evaluating the radiation-induced changes occurring in the mechanical properties of pressure vessel beltline materials.

Westinghouse has provided such a surveillance program for the Indian Point Unit No. 2 nuclear power plant. The encapsulated C_V specimens are located on the O.D. surface of the thermal shield where the fast neutron flux density is about three times that at the adjacent vessel wall surface. Therefore, the increases (shifts) in transition temperatures of the materials in the pressure vessel are generally less than the corresponding shifts observed in the surveillance specimens. However, because of azimuthal variations in neutron flux density, capsule fluences may lead or lag the maximum vessel fluence in a corresponding exposure period. For example, Capsule T (removed during the 1976 refuelling outage) was exposed to a neutron fluence approximately three times that at the maximum exposure point on the vessel I.D., while Capsule V (scheduled for removal at a later date) is receiving a neutron flux about equal to that at the point of maximum vessel exposure. The capsules also contain several dosimeter materials for experimentally determining the average neutron flux density at each capsule location during the exposure period.

The Indian Point Unit No. 2 material surveillance capsules also include tensile specimens as recommended by ASTM E 185. At the present time, irradiated tensile properties are used only to indicate that the materials tested continue to meet the requirements of the appropriate material specification. In addition, some of the material surveillance capsules contain wedge opening loading (WOL) fracture mechanics specimens. Current technology limits the testing of these specimens at temperatures well below the minimum service temperature to obtain valid fracture mechanics data per ASTM E 399[11], "Standard Method of Test for Plane-Strain Fracture Toughness of Metallic Materials." However, recent work reported by Mager and Witt[12] may lead to methods for evaluating high-toughness materials with small fracture mechanics specimens. Currently, the NRC suggests storing these specimens until an acceptable testing procedure has been defined.

This report describes the results obtained from testing the contents of Capsule T. These data are analyzed to estimate the radiation-induced changes in the mechanical properties of the pressure vessel at the time of the 1976 refuelling outage as well as predicting the changes expected to occur at selected times in the future operation of the Indian Point Unit No. 2 power plant.

III. DESCRIPTION OF MATERIAL SURVEILLANCE PROGRAM

The Indian Point Unit No. 2 material surveillance program is described in detail in WCAP 7323[13], dated May 1969. Eight materials surveillance capsules (five Type I and three Type II) were placed in the reactor vessel between the thermal shield and the vessel wall prior to startup, see Figure 1. The vertical center of each capsule is opposite the vertical center of the core. The neutron flux density at the Capsule T location leads the maximum flux density on the vessel I. D. by a factor of 2.9.[14] The Type I capsules each contain Charpy V-notch, tensile and WOL specimens machined from the three SA533 Gr B plates located at the core beltline plus Charpy V-notch specimens machined from a reference heat of steel utilized in a number of Westinghouse surveillance programs. The Type II capsules include specimens machined from weld metal and HAZ material representative of those materials in the core beltline region of the vessel as well as base plate material. Capsule T, one of the Type I capsules, was removed during the 1976 refuelling outage.

The chemistries and heat treatments of the vessel surveillance materials contained in Capsule T are summarized in Table I. All test specimens were machined from each of the materials at the quarter-thickness (1/4 T) location. The base metal C_V specimens were oriented with their long axis parallel to the primary rolling direction; the C_V notches were perpendicular to the major plate surfaces. Tensile specimens were

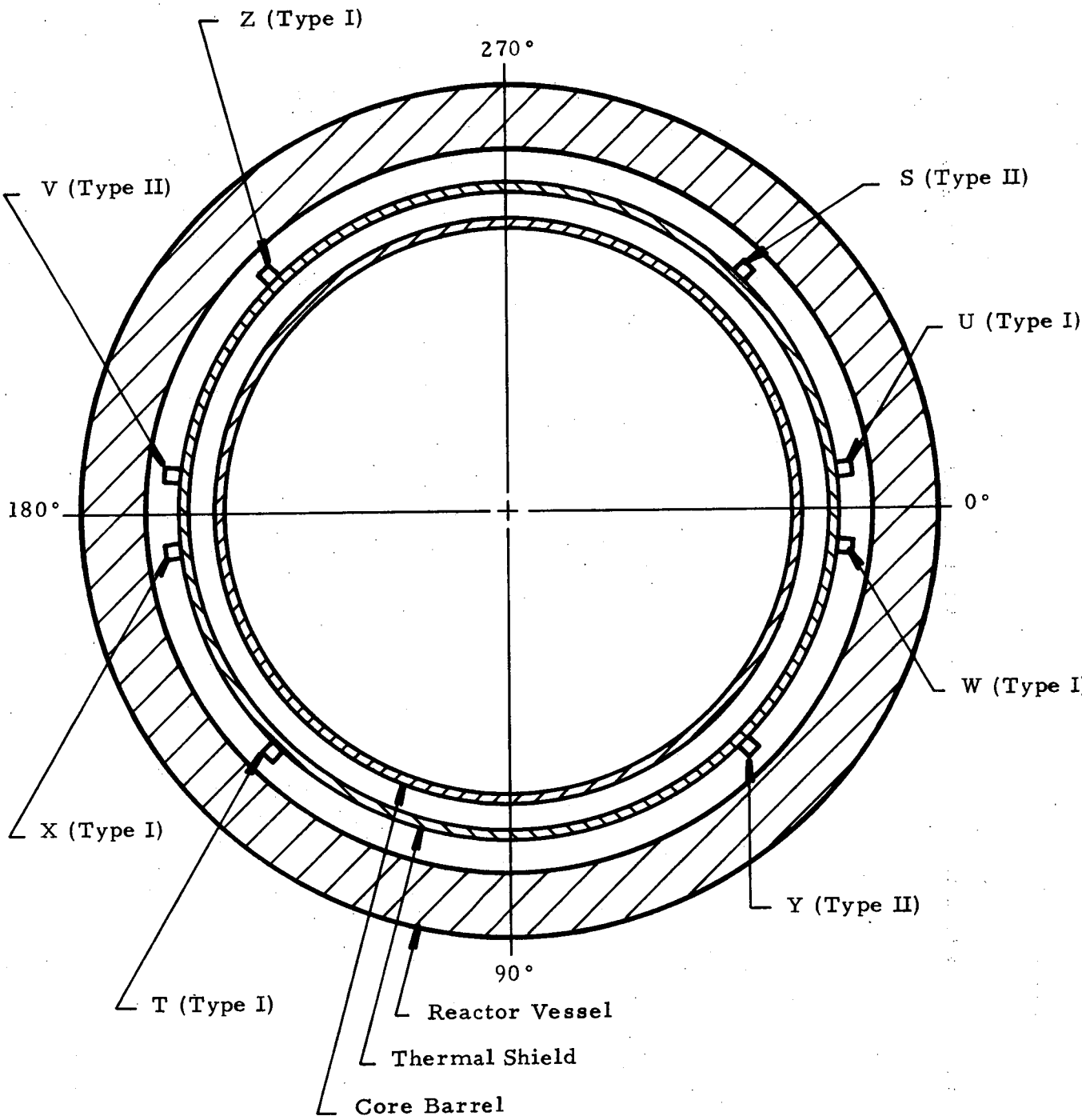

FIGURE 1. ARRANGEMENT OF SURVEILLANCE CAPSULES IN THE PRESSURE VESSEL

TABLE I

Indian Point Unit No. 2 Reactor Vessel Surveillance Materials[13]

Heat Treatment History

Shell Plate Material:

1550°-1600°F, 4 hours, water quenched
1225° ± 25°F, 4 hours, air cooled
1150° ± 25°F, 40 hours, furnace cooled to 600°F

Weldment:

1150° ± 25°F, 19.75 hours, furnace cooled to 600°F

Correlation Monitor:

1650°F, 4 hours, water quenched to 300°F
1200°F, 6 hours, air cooled

Chemical Composition (Percent)

Material	C	Mn	P	S	Si	Ni	Mo	Cu[15]
Plate B2002-1	0.20	1.28	0.010	0.019	0.25	0.58	0.46	0.25
Plate B2002-2	0.22	1.30	0.014	0.018	0.22	0.46	0.50	0.14
Plate B2002-3	0.22	1.29	0.011	0.020	0.25	0.57	0.46	0.14
Corr. Monitor	0.24	1.34	0.011	0.023	0.23	(a)	0.51	(a)
Weld Metal	(a)	(a)	(a)	(a)	(a)	(a)	(a)	(a)

(a) Not reported.

machined from the three vessel plates with the longitudinal axis parallel to the plate rolling direction. The WOL specimens were machined with the simulated crack perpendicular to the primary rolling direction and to the plate surfaces. All mechanical test specimens, see Figure 2, were taken at least one plate thickness from the quenched edges of the plate material.

Capsule T contained 32 Charpy V-notch specimens (8 each from the three vessel plate materials plus 8 from the reference steel plate); 3 tensile specimens (1 from each plate); and 6 WOL specimens (2 from each plate). The specimen numbering system and location within Capsule T is shown in Figure 3.

Capsule T also was reported to contain the following dosimeters for determining the neutron flux density:

Target Element	Form	Quantity
Copper	Bare wire	2
Nickel	Bare wire	1
Cobalt (in aluminum)	Bare wire	3
Cobalt (in aluminum)	Cd shielded wire	3

In addition, slices were taken from five C_V specimens to serve as iron dosimeters.

Three eutectic alloy thermal monitors had been inserted in holes in the steel spacers in Capsule T. Two (located top and bottom) were 2.5% Ag and 97.5% Pb with a melting point of 579 °F. The third (located at the center of the capsule) was 1.75% Ag, 0.75% Sn and 97.5% Pb having a melting point of 590 °F.

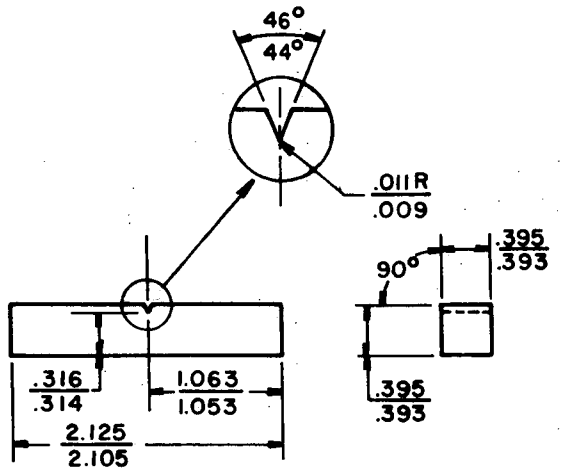

(a) Charpy V-notch Impact Specimen

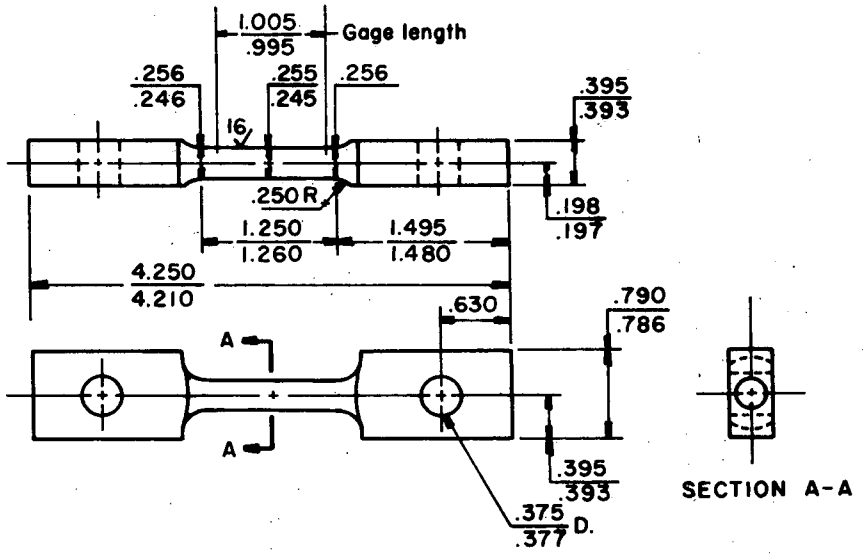

(b) Tensile Specimen

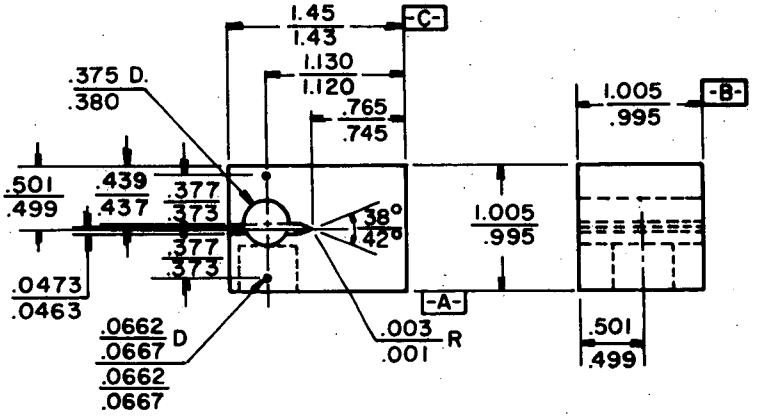

(c) Wedge Opening Loading Specimen

FIGURE 2. VESSEL MATERIAL SURVEILLANCE SPECIMENS

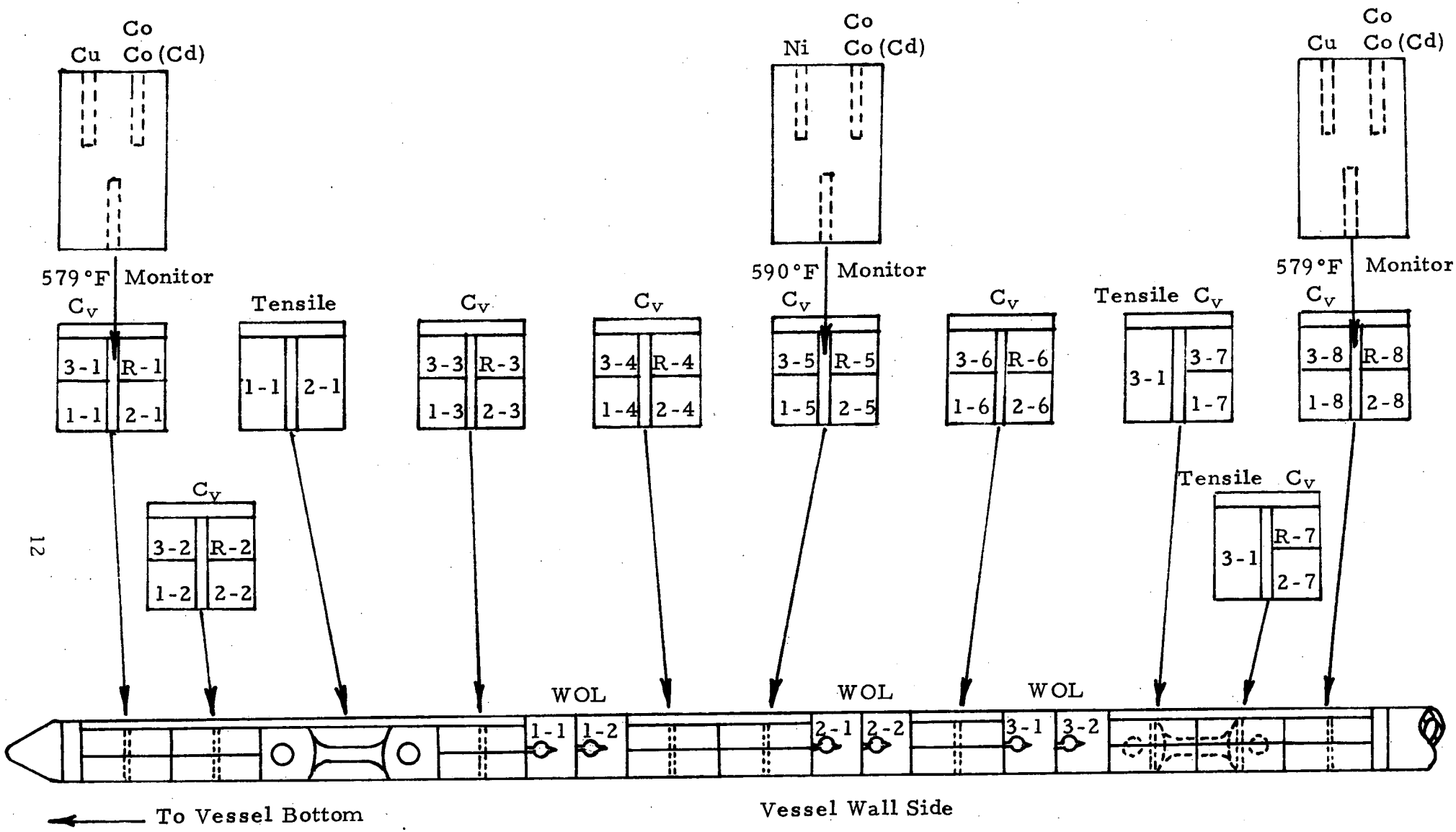

FIGURE 3. ARRANGEMENT OF SPECIMENS AND DOSIMETERS IN CAPSULE T

IV. TESTING OF SPECIMENS FROM CAPSULE T

The capsule shipment, capsule opening, specimen testing and reporting of results were carried out in accordance with the following SwRI Nuclear Project Operating Procedures:

(1) XI-MS-1, Determination of Specific Activity of Neutron Radiation Detector Specimen.

(2) XI-MS-3, Conducting Tension Tests on Metallic Materials.

(3) XI-MS-4, Charpy Impact Tests on Metallic Materials.

(4) XIII-MS-1, Opening Radiation Surveillance Capsules and Handling and Storing Specimens.

(5) XI-MS-5, Conducting Wedge-Opening-Loading Tests on Metallic Materials.

(6) XI-MS-6, Determination of Specific Activity of Neutron Radiation Fission Monitor Detector Specimens.

Copies of the above documents are on file at SwRI.

Southwest Research Institute utilized a procedure which had been prepared for the 1976 refuelling outage for the removal of Capsule T from the reactor vessel and the shipment of the capsule to the SwRI laboratories. SwRI contracted with Todd Shipyards - Nuclear Division to supply appropriate cutting tools and a licensed shipping cask. Todd personnel severed the capsule from its extension tube, sectioned the extension tube into three-foot lengths, supervised the loading of the capsule and extension tube materials into the shipping cask, and transported the cask to San Antonio.

The capsule shell had been fabricated by making two long seam welds to join two half-shells together. The long seam welds were milled off on a Bridgeport vertical milling machine set up in one hot cell. Before milling off the long seam weld beads, transverse saw cuts were made to remove the two capsule ends. After the long seam welds had been milled away, the top half of the capsule shell was removed. The specimens and spacer blocks were carefully removed and placed in an indexed receptacle so that capsule location was identifiable. After the disassembly had been completed, the specimens were carefully checked for identification and location, as listed in WCAP 7323.[13]

Each specimen was inspected for identification number, which was checked against the master list in WCAP 7323. No discrepancies were found. The thermal monitors and dosimeter wires were removed from the holes in the spacers. The thermal monitors, contained in quartz vials, were examined and no evidence of melting was observed, thus indicating that the maximum temperature during exposure of Capsule T did not exceed 579 °F.

The specific activities of the dosimeters were determined at SwRI with an NDC 2200 multichannel analyzer and an NaI(Th) 3 x 3 scintillation crystal. The calibration of the equipment was accomplished with appropriate standards and an interlaboratory cross check with two independent counting laboratories on ^{60}Co-, ^{54}Mn- and ^{58}Co-containing dosimeter wires. All activities were corrected to the time-of-removal (TOR) at reactor shutdown.

Infinitely dilute saturated activities (A_{SAT}) were calculated for each of the dosimeters because A_{SAT} is directly related to the product of the energy-dependent microscopic activation cross section and the neutron flux density. The relationship between A_{TOR} and A_{SAT} is given by:

$$\frac{A_{TOR}}{A_{SAT}} = \sum_{m=1}^{m=n} (1 - e^{-\lambda T_m})(e^{-\lambda t_m})$$

where: λ = decay constant for the activation product, day^{-1};

T_m = equivalent operating days at 2758 MwTh for operating period m;

t_m = decay time after operating period m, days.

An alternate expression which gives equivalent results is:

$$\frac{A_{TOR}}{A_{SAT}} = \sum_{m=1}^{m=n} P_m (1 - e^{-\lambda T_o})(e^{-\lambda t_m})$$

where: T_o = operating days;

P_m = average fraction of full power during operating period.

The Indian Point Unit No. 2 operating history up to the 1976 refuelling shutdown is presented in Table II. The specific time of release and specific saturated activities for each dosimeter are presented in Table III.

The primary result desired from the dosimeter analysis is the total fast neutron fluence (> 1 MeV) which the surveillance specimens received.

TABLE II

Summary of Reactor Operations
Indian Point Unit No. 2

Period (m)	Dates Start	Dates Stop	Shutdown Days	Operating Days, T_m	Decay Time After Period, t_m	Fraction of Full Power in Period, P_m
1	08-15-73	08-24-73	-	10	949	0.4377
	08-25-73	08-25-73	1	-		
2	08-26-73	09-07-73	-	13	935	0.4532
	09-08-73	09-20-73	13	-		
3	09-21-73	09-28-73	-	8	914	0.3161
	09-29-73	09-30-73	2	-		
4	10-01-73	10-12-73	-	12	900	0.3088
	10-13-73	01-25-74	105	-		
5	01-26-74	01-29-74	-	4	791	0.2412
	01-30-74	03-21-74	51	-		
6	03-22-74	04-18-74	-	28	712	0.5438
	04-19-74	04-28-74	10	-		
7	04-29-74	05-03-74	-	5	697	0.4962
	05-04-74	05-04-74	1	-		
8	05-05-74	05-10-74	-	6	690	0.4743
	05-11-74	05-12-74	2	-		
9	05-13-74	05-13-74	-	1	687	0.0730
	05-14-74	05-20-74	7	-		
10	05-21-74	06-14-74	-	25	655	0.6653
	06-15-74	06-16-74	2	-		
11	06-17-74	07-22-74	-	36	617	0.7691
	07-23-74	07-23-74	1	-		
12	07-24-74	07-26-74	-	3	613	0.7593
	07-27-74	08-05-74	10	-		
13	08-06-74	09-06-74	-	32	571	0.6653
	09-07-74	09-09-74	3	-		

(Continued)

TABLE II (Cont'd.)

Period (m)	Dates Start	Dates Stop	Shutdown Days	Operating Days, T_m	Decay Time After Period, t_m	Fraction of Full Power in Period, P_m
14	09-10-74	09-30-74	-	21	547	0.7429
	10-01-74	10-11-74	11	-		
15	10-12-74	11-09-74	-	29	507	0.8657
	11-10-74	11-10-74	1	-		
16	11-11-74	12-06-74	-	26	480	0.8306
	12-07-74	12-07-74	1	-		
17	12-08-74	01-01-75	-	25	454	0.8495
	01-02-75	01-04-75	3	-		
18	01-05-75	01-05-75	-	1	450	0.5450
	01-06-75	01-06-75	1	-		
19	01-07-75	01-31-75	-	25	424	0.8810
	02-01-75	02-02-75	2	-		
20	02-03-75	02-28-75	-	26	396	0.9408
	03-01-75	04-03-75	34	-		
21	04-04-75	05-02-75	-	29	333	0.7652
	05-03-75	05-03-75	1	-		
22	05-04-75	07-28-75	-	86	246	0.9114
	07-29-75	08-10-75	13	-		
23	08-11-75	09-12-75	-	33	200	0.7108
	09-13-75	09-13-75	1	-		
24	09-14-75	10-16-75	-	33	166	0.7962
	10-17-75	10-29-75	13	-		
25	10-30-75	11-14-75	-	16	137	0.7467
	11-15-75	11-15-75	1	-		
26	11-16-75	01-04-76	-	50	86	0.8427
	01-05-76	01-05-76	1	-		
27	01-06-76	01-29-76	-	24	61	0.8703
	01-30-76	02-04-76	6	-		
28	02-05-76	03-30-76	-	55	0	0.9122

Total Power Generation = 517.749 Effective Full Power Days
(includes 5.749 EFPD accumulated before 08-15-73)

TABLE III

Summary of Neutron Dosimetry Results
Capsule T

Monitor Identification	Activation Reaction	Measured Activity (dps/mg)	Saturated Activity (dps/mg)
R1[a]	$^{54}Fe(n, p)^{54}Mn$	1.57×10^3	2.72×10^3
R3[a]	"	1.66×10^3	2.88×10^3
R4[a]	"	1.59×10^3	2.77×10^3
R6[a]	"	1.59×10^3	2.77×10^3
R8[a]	"	1.49×10^3	2.58×10^3
	Avg.	1.58×10^3	2.75×10^3
Cu (Top)	$^{63}Cu(n,\alpha)^{60}Co$	5.28×10^2	3.25×10^3
Cu (Bottom)	"	4.53×10^2	2.79×10^3
Ni (Center)	$^{58}Ni(n, p)^{58}Co$	3.69×10^5	4.68×10^5
Co (Top)	$^{59}Co(n, \gamma)^{60}Co$	5.00×10^7	3.08×10^8
Co-Cd (Top)	"	2.36×10^7	1.46×10^8
Co (Center)	"	5.66×10^7	3.49×10^8
Co-Cd (Center)	"	2.24×10^7	1.38×10^8
Co (Bottom)	"	5.14×10^7	3.16×10^8
Co-Cd (Bottom)	"	2.31×10^7	1.42×10^8

(a) Charpy specimen from which sample was removed.

The average flux density at full power is given by:

$$\varphi = \frac{A_{SAT}}{N_0 \bar{\sigma}}$$

where: φ = energy-dependent neutron flux density, n/cm^2-sec;

A_{SAT} = saturated activity, dps/mg target element;

$\bar{\sigma}$ = spectrum-averaged activation cross section, cm^2;

N_0 = number of target atoms per mg.

The total neutron fluence is then equal to the product of the average neutron flux density and the equivalent reactor operating time at full power.

The neutron flux density was calculated from the $^{54}Fe(n, p)^{54}Mn$ reaction because it has a high energy threshold and the energy response is well known. The energy spectrum for Capsule T was calculated with the DOT 3.5 two-dimensional discrete ordinates transport code with a 22 group neutron cross section library, a P_1 expansion of the scattering matrix and an S_8 order of angular quadrature. The normalized spectrum for Capsule T and the group-organized cross sections for the $^{54}Fe(n, p)^{54}Mn$ reaction derived from the ENDF/B-IV library[16] are given in Table IV. The value of $\bar{\sigma}_{Fe}$ is given by:

$$\bar{\sigma}_{Fe}\ (> 1\ MeV) = \frac{\int_{1.10}^{10\ MeV} \sigma_{Fe}(E)\varphi(E)\,dE}{\int_{1.00}^{10\ MeV} \varphi(E)\,dE}$$

where: $\bar{\sigma}_{Fe}\ (> 1\ MeV)$ = the calculated spectrum-averaged cross section for flux > 1 MeV, cm^2 determined for the $^{54}Fe(n, p)^{54}Mn$ reaction.

TABLE IV

Fast Neutron Spectrum and Iron Activation
Cross Sections for Capsule T

Energy Range (MeV)	Normalized Neutron Flux	$^{54}Fe(n, p)^{54}Mn$ Cross Section (barns)
8.18 - 10.0	0.0105	0.581
6.36 - 8.18	0.0284	0.577
4.96 - 6.36	0.0535	0.491
4.06 - 4.96	0.0535	0.354
3.01 - 4.06	0.0925	0.205
2.35 - 3.01	0.1451	0.099
1.83 - 2.35	0.1705	0.023
1.11 - 1.83	0.4459	0.0014

$$\bar{\sigma}_{Fe} = 0.097 \text{ barns}$$

The resulting value obtained for fast (> 1 MeV) neutron flux density at the Capsule T location was 4.51×10^{10} neutrons/cm^2-sec. Since Indian Point Unit No. 2 operated for an equivalent of 518 full power days up to the 1976 refuelling outage, the total neutron fluence for Capsule T is equal to 2.02×10^{18} neutrons/cm^2 (E > 1 MeV).

The irradiated Charpy V-notch specimens were tested on a SATEC impact machine. The test temperatures were selected to develop the ductile-brittle transition and upper shelf regions. The unirradiated Charpy V-notch impact data reported by Westinghouse[13] and the data obtained by SwRI on the specimens contained in Capsule T are presented in Tables V through VIII. The Charpy V-notch transition curves for the three plate materials and the correlation monitor material are presented in Figures 4 through 7. The radiation-induced shift in transition temperatures for the vessel plates are indicated at 77 ft-lb and 54 mil lateral expansion because the specimens are longitudinally oriented. A summary of the shifts in RT_{NDT} and C_v upper shelf energies for each material are presented in Table IX.

Tensile tests were carried out in the SwRI hot cells using a Dillon 10,000-lb capacity tester equipped with a strain gage extensometer, load cell and autographic recording equipment. All of the tensile specimens were tested at 550°F. The results, along with tensile data reported by Westinghouse on the unirradiated materials[13], are presented in Table X. The load-strain records are included in Appendix A.

TABLE V

Charpy V-Notch Impact Data
Indian Point Unit No. 2 Pressure Vessel Shell Plate B2002-1

Condition	Spec. No.	Temp. (°F)	Energy (ft-lbs)	Shear (%)	Lateral Expansion (mils)
Baseline	(a)	-40	10.0	10	8
		-40	9.0	10	6
		-40	8.0	10	7
		-20	19.0	15	15
		-20	14.5	15	16
		-20	8.5	15	8
		0	21.5	25	18
		0	33.5	25	28
		0	34.0	25	29
		10	40.5	30	32
		10	36.0	25	28
		10	35.5	25	27
		60	68.5	45	54
		60	62.0	45	49
		60	50.5	40	40
		110	88.0	65	70
		110	69.5	60	56
		110	77.0	60	61
		160	116.5	98	84
		160	122.0	98	86
		160	112.0	95	85
		210	111.0	100	83
		210	121.5	100	88
		210	119.0	100	83
Capsule T	1-6	40	27.0	5	23
	1-1	78	38.5	10	33
	1-5	120	53.5	15	44
	1-7	140	52.0	20	47
	1-3	160	69.0	60	56
	1-8	180	69.5	60	61
	1-2	210	95.5	95	81
	1-4	300	99.5	100	81

(a) Not reported.

TABLE VI

Charpy V-Notch Impact Data
Indian Point Unit No. 2 Pressure Vessel Shell Plate B2002-2

Condition	Spec. No.	Temp. (°F)	Energy (ft-lbs)	Shear (%)	Lateral Expansion (mils)
Baseline	(a)	-40	6.5	10	4
		-40	8.0	10	6
		-40	7.5	10	6
		-20	18.0	10	18
		-20	9.0	10	7
		-20	10.0	10	7
		10	20.0	25	19
		10	42.5	30	34
		10	14.0	25	14
		30	37.5	30	32
		30	41.0	35	35
		30	49.5	30	41
		60	73.5	40	58
		60	49.0	40	39
		60	59.5	40	50
		110	80.5	65	60
		110	76.0	60	60
		110	91.0	65	70
		160	108.0	85	84
		160	120.5	95	85
		160	118.0	95	84
		210	112.0	100	80
		210	120.5	100	83
		210	115.0	100	82
Capsule T	2-1	78	10.0	5	9
	2-6	100	43.0	10	44
	2-5	120	22.5	5	18
	2-7	140	63.0	35	49
	2-3	160	65.0	70	57
	2-8	180	97.5	80	53
	2-2	210	103.0	100	85
	2-4	300	88.0	100	72

(a) Not reported.

TABLE VII

Charpy V-Notch Impact Data
Indian Point Unit No. 2 Pressure Vessel Shell Plate B2002-3

Condition	Spec. No.	Temp. (°F)	Energy (ft-lbs)	Shear ( )	Lateral Expansion (mils)
Baseline	(a)	-40	6.5	10	4
		-40	8.0	10	5
		-40	6.0	10	7
		-20	25.5	20	20
		-20	14.0	15	12
		-20	11.0	15	7
		10	41.5	25	33
		10	17.0	25	14
		10	37.5	25	29
		30	34.0	35	30
		30	45.5	35	36
		30	42.5	35	36
		60	54.5	40	45
		60	51.5	40	39
		60	41.0	40	33
		110	71.0	60	60
		110	79.5	70	62
		110	83.5	70	62
		160	116.5	99	83
		160	110.0	95	80
		160	95.5	90	76
		210	109.0	90	80
		210	113.5	100	78
		210	113.0	100	82
Capsule T	3-1	78	20.0	5	16
	3-3	160	34.5	20	28
	3-8	180	40.5	10	30
	3-2	210	53.0	35	46
	3-7	260	88.0	100	76
	3-4	300	88.0	100	72
	3-5	350	92.5	100	80
	3-6	400	89.5	100	82

(a) Not reported.

TABLE VIII

Charpy V-Notch Impact Data
Correlation Monitor Material (Supplied by U. S. Steel)

Condition	Spec. No.	Temp. (°F)	Energy (ft-lbs)	Shear (%)	Lateral Expansion (mils)
Baseline	(a)	-150	12.5	10	10
		-150	10.5	15	11
		-100	35.0	25	29
		-100	9.0	20	9
		-100	18.0	30	19
		-80	13.0	20	12
		-80	32.5	20	27
		-80	26.0	20	23
		-40	34.0	30	30
		-40	35.5	35	31
		-40	48.0	35	40
		10	78.5	60	64
		10	74.0	60	60
		10	81.0	70	68
		60	102.5	80	78
		60	102.0	85	82
		60	100.0	85	80
		110	112.5	99	88
		110	108.5	90	87
		110	108.5	98	88
		160	115.5	100	90
		160	113.0	100	92
		160	120.0	100	93
		210	121.0	100	92
		210	123.5	100	91
		210	117.5	100	92
Capsule T	R5	40	9.5	nil	9
	R1	78	20.5	5	18
	R6	100	31.0	10	27
	R4	120	35.5	15	32
	R7	140	79.5	100	66
	R3	160	49.0	70	41
	R8	180	52.5	60	40
	R2	210	68.0	100	60

(a) Not reported.

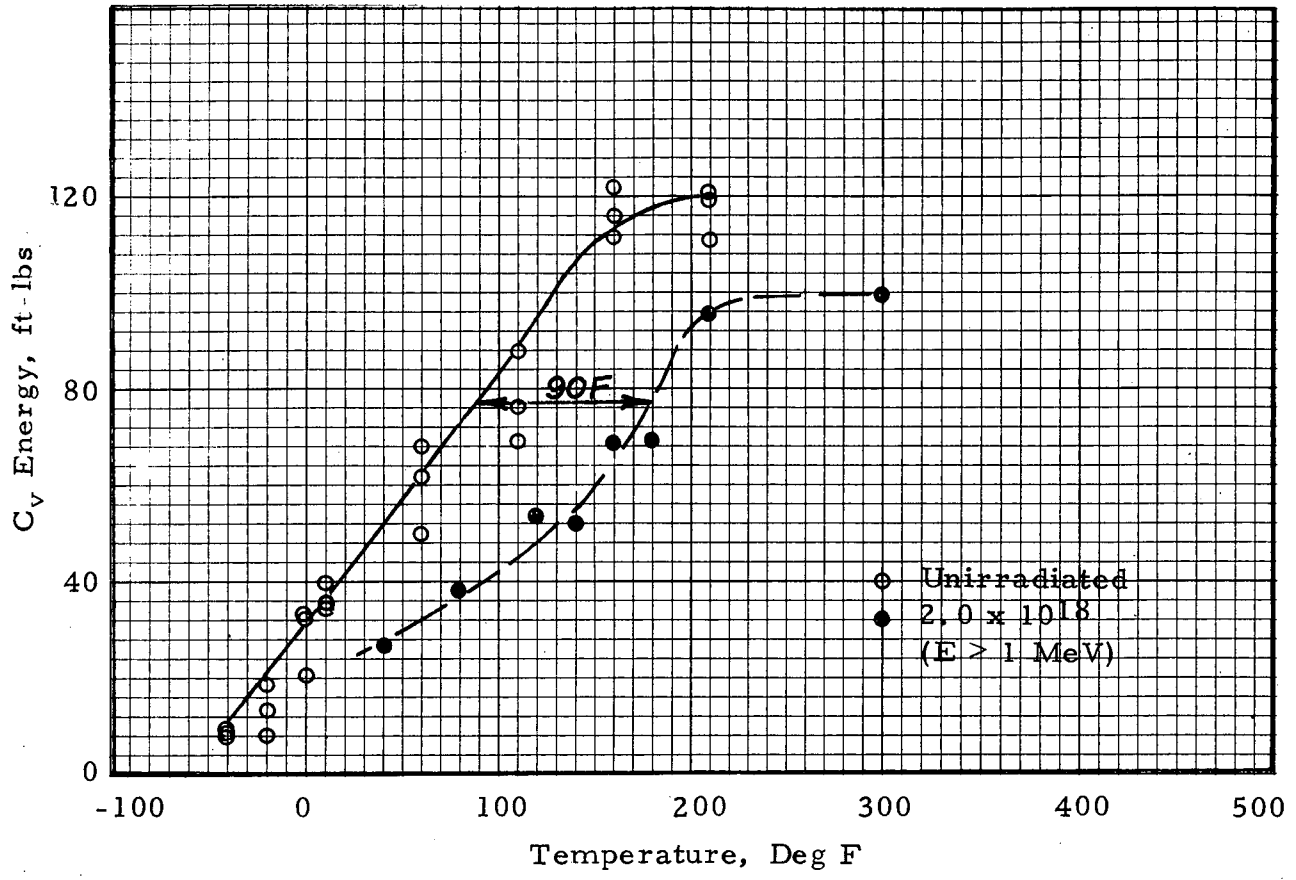

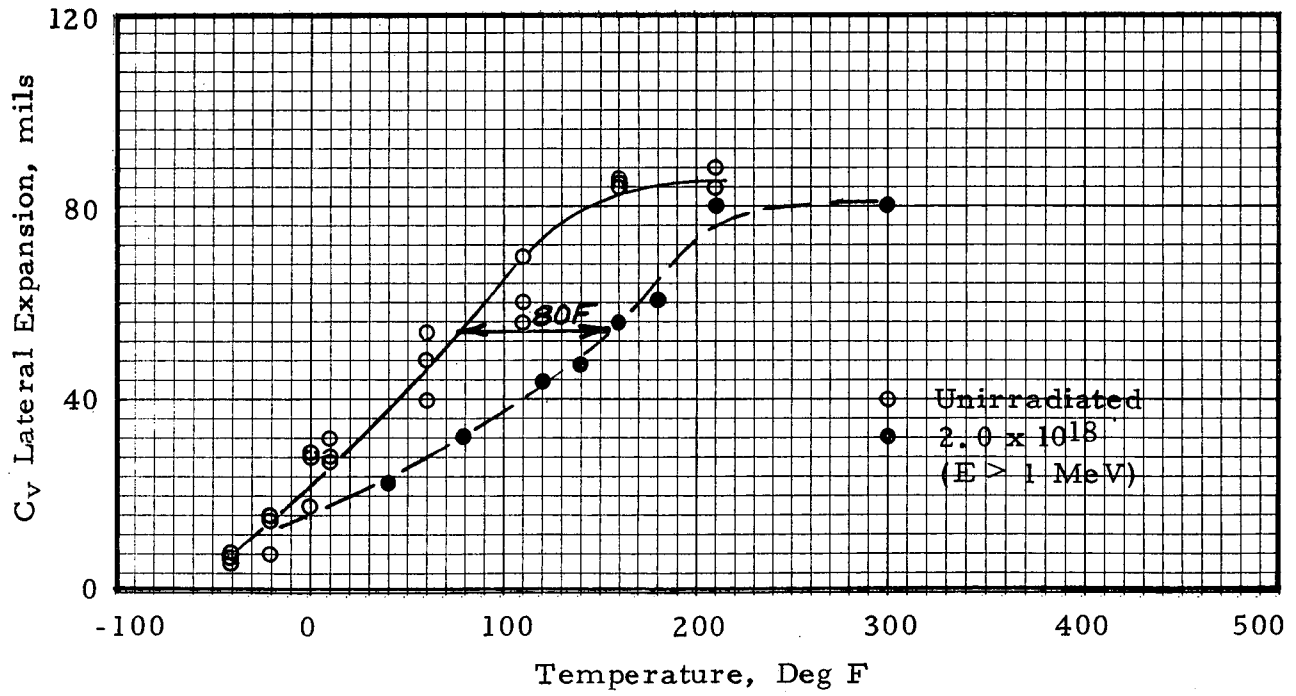

FIGURE 4. EFFECT OF IRRADIATION ON C_v IMPACT PROPERTIES OF INDIAN POINT UNIT NO. 2 SHELL PLATE B2002-1

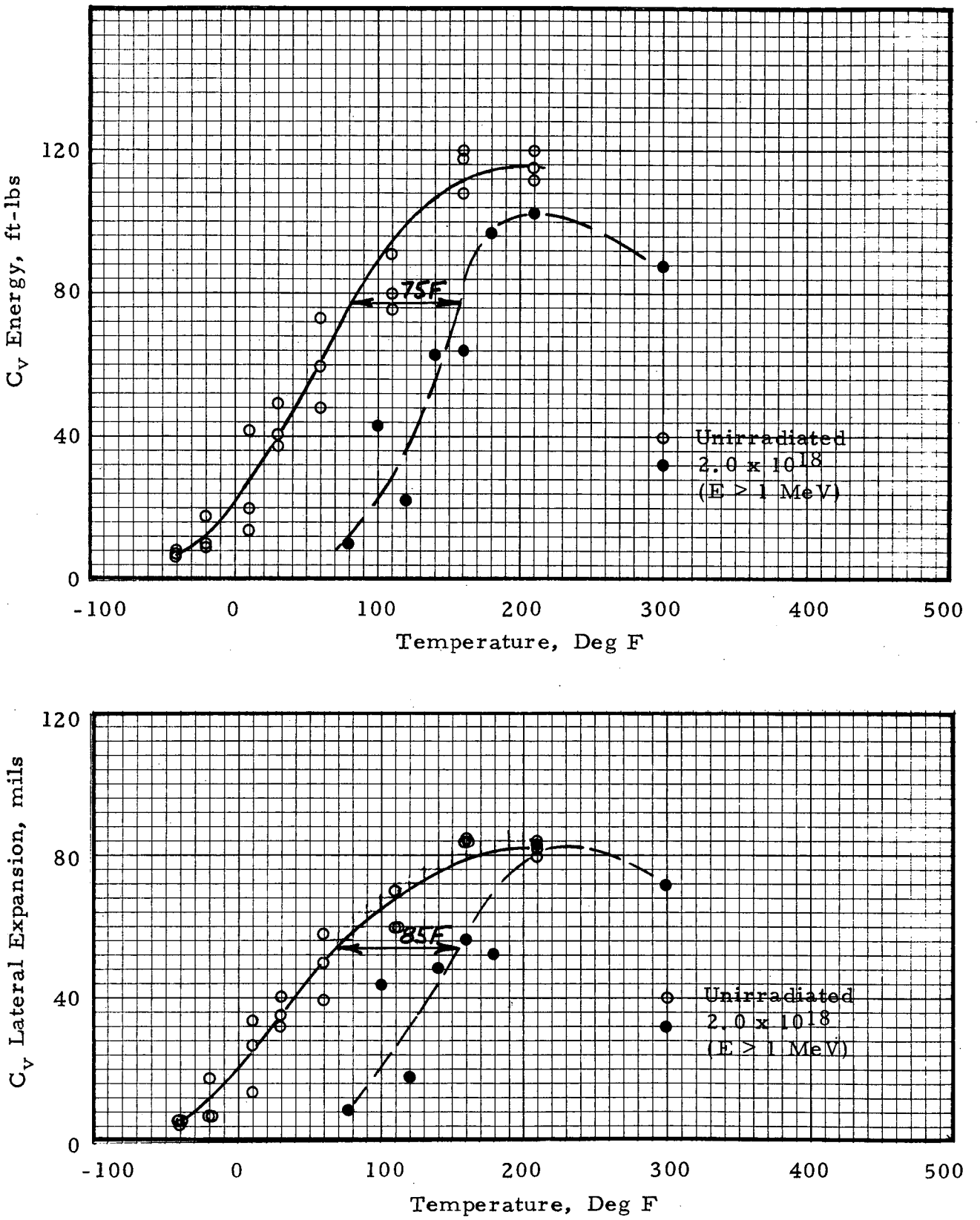

FIGURE 5. EFFECT OF IRRADIATION ON C_v IMPACT PROPERTIES OF INDIAN POINT UNIT NO. 2 SHELL PLATE B2002-2

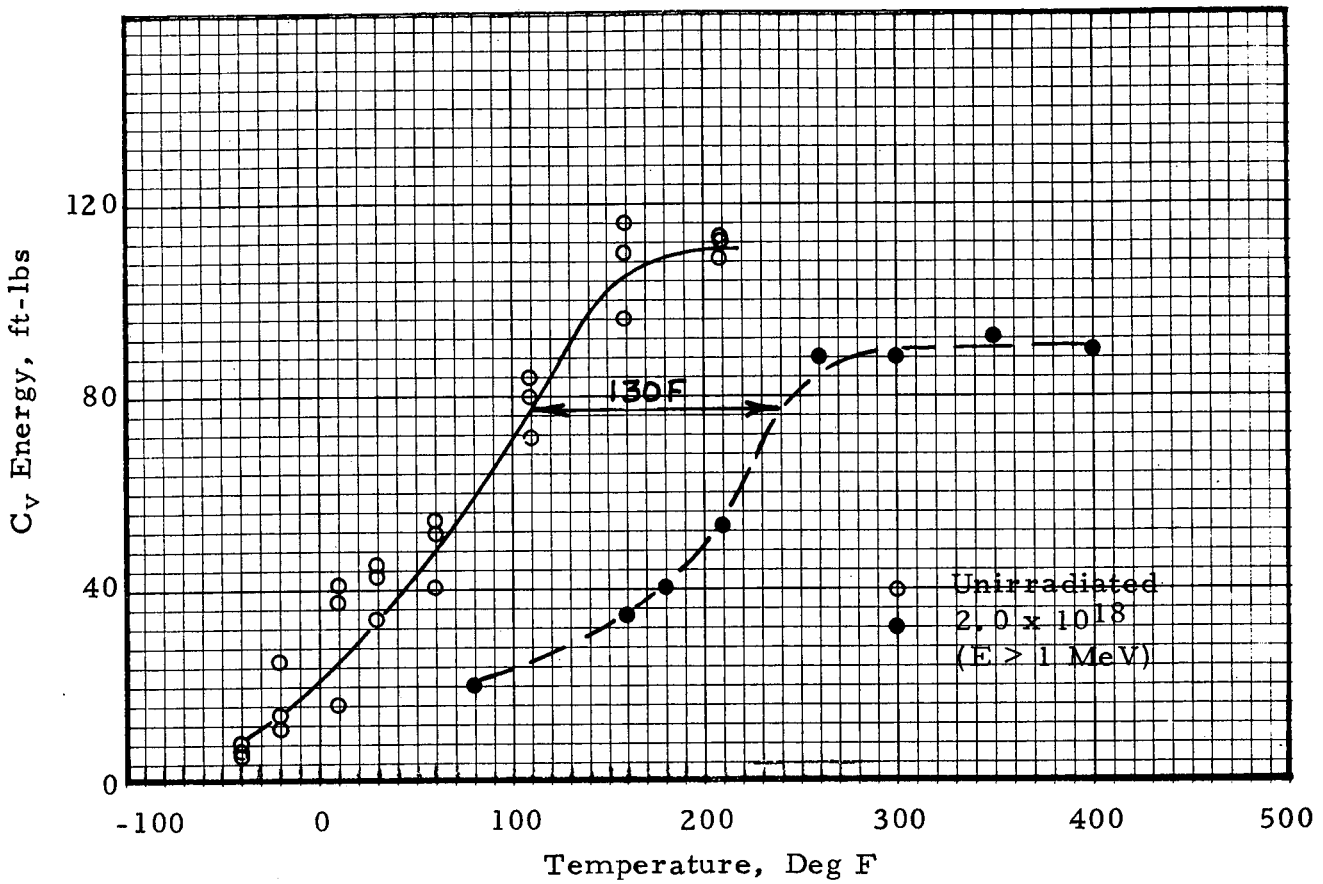

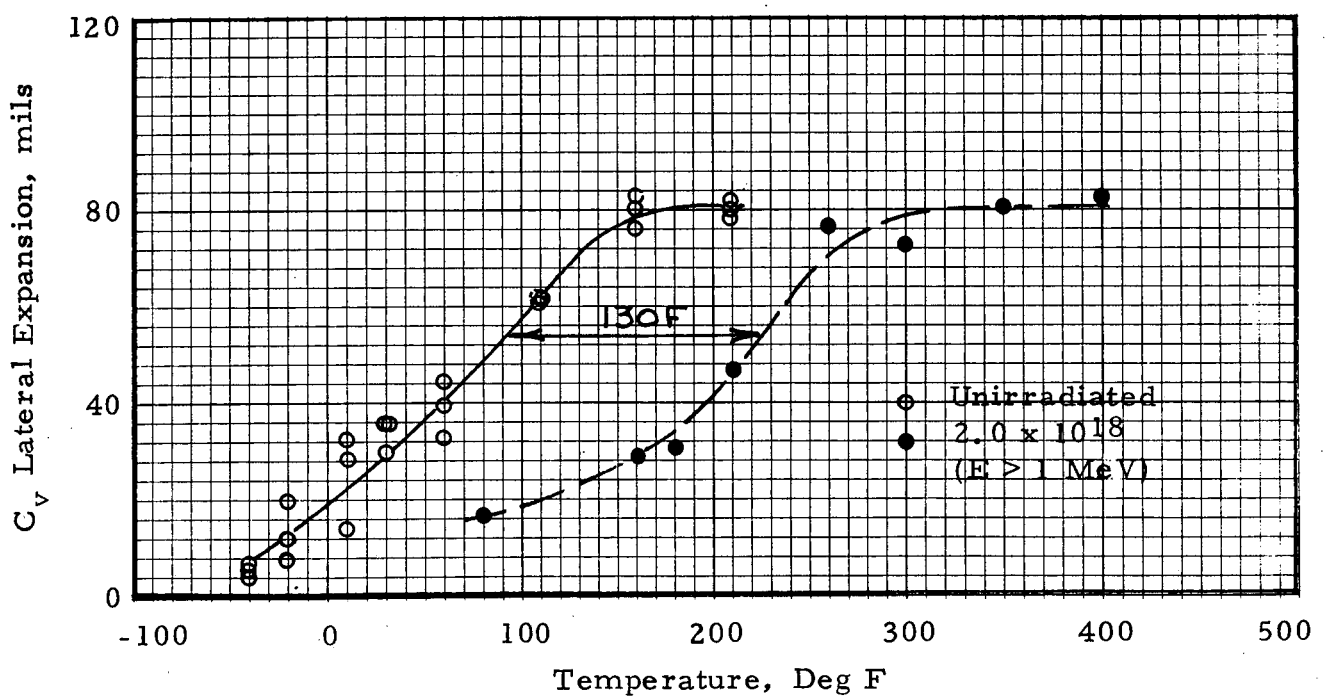

FIGURE 6. EFFECT OF IRRADIATION ON C_v IMPACT PROPERTIES OF INDIAN POINT UNIT NO. 2 SHELL PLATE B2002-3

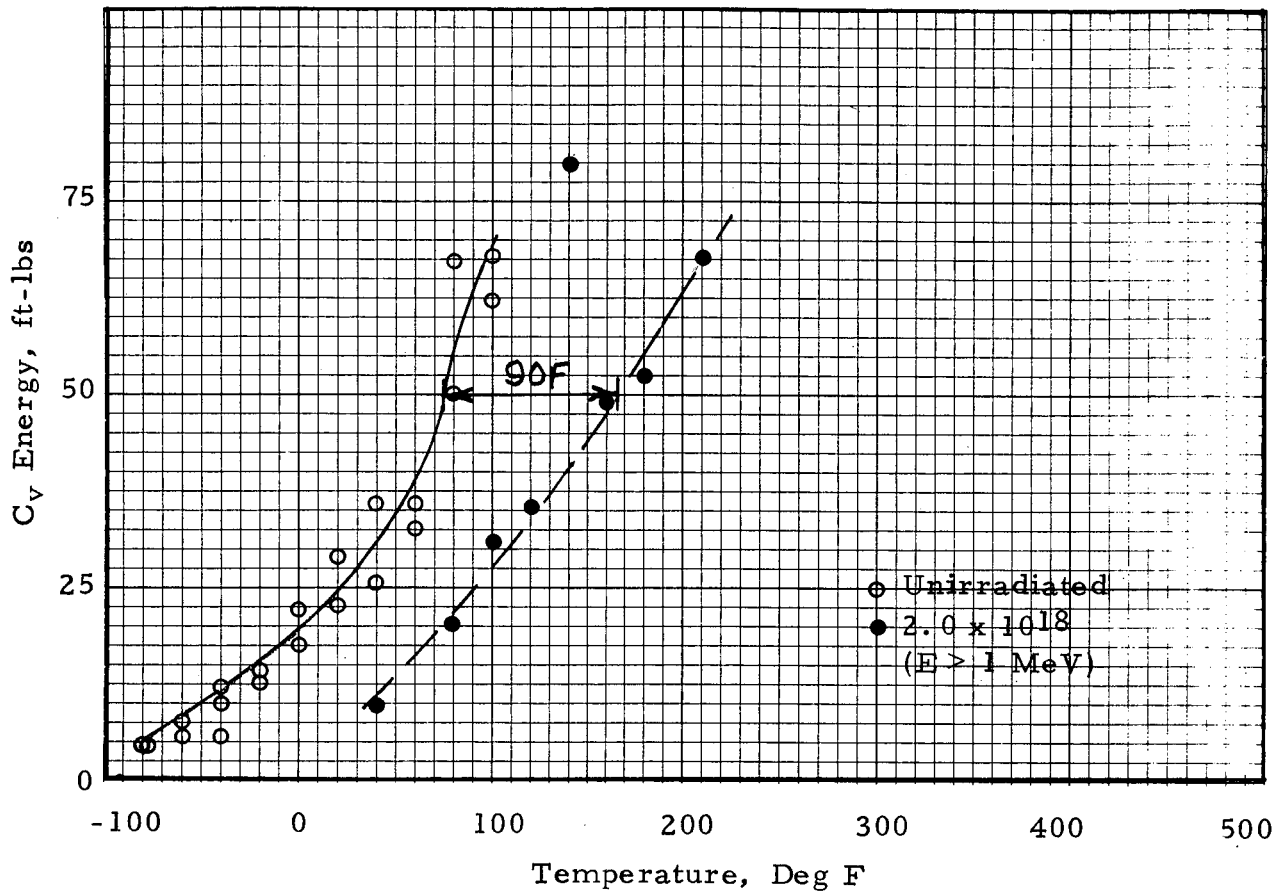

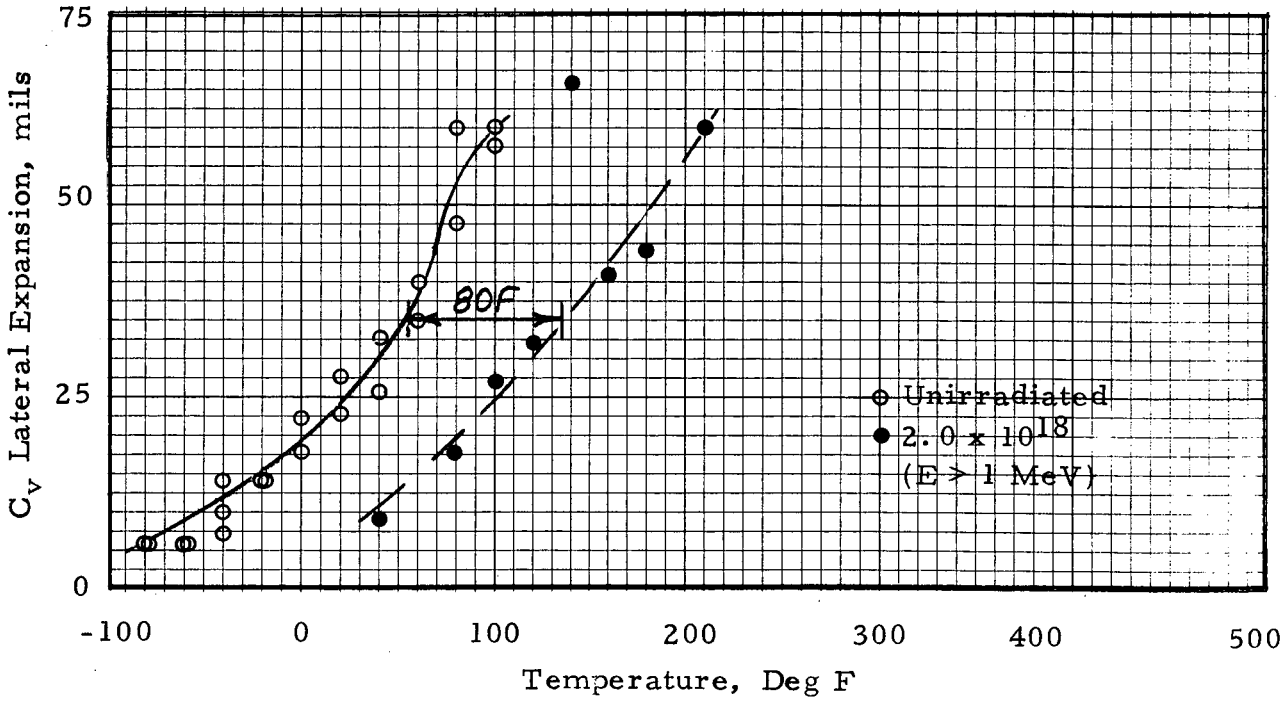

FIGURE 7. EFFECT OF IRRADIATION ON C_v IMPACT PROPERTIES OF INDIAN POINT UNIT NO. 2 CORRELATION MONITOR MATERIAL

TABLE IX

Notch Toughness Properties of Capsule T Specimens
Indian Point Unit No. 2

	Plate B2002-1[1]	Plate B2002-2[2]	Plate B2002-3[3]	Correlation Monitor[4]
77 ft-lb C_V Temp. (deg F)				
Irradiated	178	158	240	165
Unirradiated	88	83	110	75
ΔT	90	75	130	90
54 mil C_V Temp. (deg F)				
Irradiated	157	152	225	135
Unirradiated	77	67	95	55
ΔT	80	85	130	80
C_V Upper Shelf Energy (ft-lb)				
Unirradiated	117	116	113	116
Irradiated	99.5	103	88	68
ΔE, ft-lbs	17.5	13	25	48
ΔE, %	15	11	22	41

(1) 0.16% Copper
(2) 0.17% Copper
(3) 0.25% Copper
(4) Energy transition at 50 ft-lb
Lateral expansion transition at 35 mil

TABLE X

Tensile Properties of Surveillance Materials
Capsule T

Condition	Specimen Ident.	Test Temp. (°F)	0.2% Yield Strength (psi)	Tensile Strength (psi)	Total Elongation (%)	Reduction in Area (%)
Baseline	B2002-1	Room	68,500	89,000	25.1	67.8
		Room	65,850	87,800	25.3	67.4
		200	61,550	79,900	24.1	68.6
		200	67,950	89,400	23.8	67.6
		400	57,900	79,900	23.1	64.7
		400	59,800	82,200	22.2	67.8
		600	56,750	80,550	21.9	64.3
		600	57,750	85,700	22.9	64.2
Capsule T	1-1	550	71,100	96,200	20.4	55.5
Baseline	B2002-2	Room	62,350	83,800	27.1	70.0
		Room	66,750	90,500	28.2	69.6
		200	63,650	84,450	24.8	70.5
		200	63,200	83,800	25.5	67.3
		400	53,800	77,900	23.1	68.5
		400	52,650	73,150	22.4	67.6
		600	53,500	78,800	22.7	64.4
		600	54,700	81,450	24.7	64.4
Capsule T	2-1	550	58,600	85,900	20.7	64.8
Baseline	B2002-3	Room	65,650	87,300	27.6	67.3
		Room	65,000	87,350	24.8	66.7
		200	67,800	88,900	23.4	68.6
		200	67,700	89,150	22.1	64.9
		400	57,950	79,550	22.3	68.7
		400	55,350	77,100	23.2	64.9
		600	57,750	83,850	24.9	68.2
		600	58,350	86,500	24.9	64.7
Capsule T	3-1	550	63,100	89,400	20.2	63.1

Testing of the WOL specimens was deferred at the request of Consolidated Edison Company. The specimens are in storage at the SwRI radiation laboratory.

The Charpy V-notch results indicate that Plate B2002-3 is more sensitive to radiation embrittlement than Plates B2002-1 and B2002-2, in opposition to the expectation that Plate B2002-1 would be the most sensitive because it was reported to have the highest copper content.[15] Check analyses for copper content were carried out on seven broken Charpy V-notch specimens, using an X-ray fluorescence technique meeting the requirements of ASTM E 322[17], with the following results:

Plate No.	Specimen No.	% Copper
B2002-1	1-2	0.17
B2002-1	1-3	0.15
B2002-2	2-2	0.18
B2002-2	2-3	0.17
B2002-3	3-2	0.27
B2002-3	3-3	0.23
Correlation Monitor	R-2	0.25

These results correlate with the Charpy V-notch impact data.

The tensile properties of Plate B2002-1 appeared to be the most affected by the radiation exposure in Capsule T. Check analyses for copper on three tested tensile specimens gave the following results:

Plate No.	Specimen No.	% Copper
B2002-1	1-1	0.21
B2002-2	2-1	0.13
B2002-3	3-1	0.09

These results correlate with the observed tensile test data. It is not known why the copper content of the test specimens is different from the reported copper content of the reactor vessel plates.

V. ANALYSIS OF RESULTS

The analysis of data obtained from surveillance program specimens has the following goals:

(1) Estimate the period of time over which the properties of the vessel beltline materials will meet the fracture toughness requirements of Appendix G of 10CFR50. This requires a projection of the measured reduction in C_V upper shelf energy to the vessel wall using knowledge of the energy and spatial distribution of the neutron flux and the dependence of C_V upper shelf energy on the neutron fluence.

(2) Develop heatup and cooldown curves to describe the operational limitations for selected periods of time. This requires a projection of the measured shift in RT_{NDT} to the vessel wall using knowledge of the dependence of the shift in RT_{NDT} on the neutron fluence and the energy and spatial distribution of the neutron flux.

The energy and spatial distribution of the neutron flux for Indian Point Unit No. 2 was calculated for Capsule T with the DOT 3.5 discrete ordinates transport code. The lead factor for Capsule T reported by Westinghouse is 2.9 for the vessel I.D. surface. This was supported by the SwRI DOT 3.5 analysis. This analysis also predicted that the fast flux at the 1/4 T and 3/4 T positions in the pressure vessel wall would be 50% and 8.5%, respectively, of that at the vessel I.D. These figures are in good agreement with fluence attenuation determinations of 46% and 10% for an 8-in. steel plate by the Naval Research Laboratory.[18] However, currently the NRC

prefers to use more conservative figures of 60% and 15%, respectively, for the attenuation of fast neutron flux at the 1/4 T and 3/4 T positions in an 8-in. vessel wall.[19] This conservatism allows for the increased fraction of neutrons which might accrue in the 0.1 to 1.0 MeV range in deep penetration situations.

A method for estimating the reduction in C_V upper shelf energy as a function of neutron fluence is given in Regulatory Guide 1.99, Revision 1.[7] However, it has been suggested[9] that a square root of fluence dependence fits existing data better. The results from Capsule T are compared to a portion of Figure 2 of Regulatory Guide 1.99, Revision 1, in Figure 8. The embrittlement response of Plate B2002-3, the most sensitive of the three plates, is in good agreement with the prediction of Regulatory Guide 1.99, Revision 1.

The projection of the C_V shelf energy of base Plate B2002-3 is complicated by the fact that the surveillance specimens are all oriented in the "strong" direction and the 50 ft-lb lower limit of 10CFR50 Appendix G applies to "weak" direction properties. In a method established by Westinghouse[20], the estimated upper shelf energy in the "weak" direction is taken to be 65% of that in the "strong" direction. Therefore, the unirradiated C_V shelf energy of Plate B2002-3 is estimated to be 73.5 ft-lbs, and this material could sustain a reduction in shelf energy of 32% before reaching 50 ft-lbs. Using the dashed curve drawn through the data point for Plate B2002-3, it is predicted that the C_V shelf energy of Plate B2002-3 will reach 50 ft-lbs at a fluence of about 9.5×10^{18} ($E > 1$ MeV). This corresponds to approximately

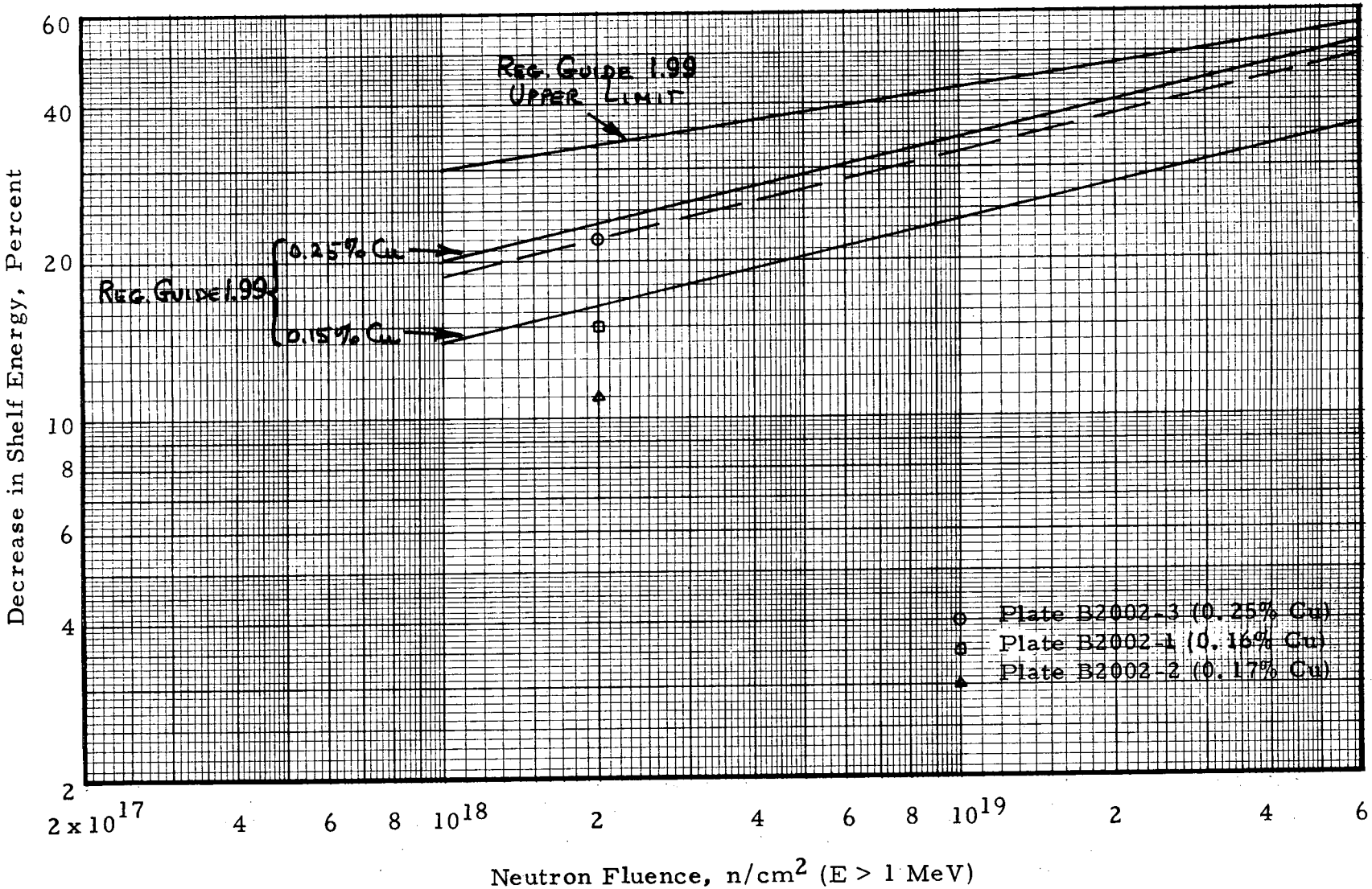

FIGURE 8. DEPENDENCE OF C_v SHELF ENERGY ON NEUTRON FLUENCE, INDIAN POINT UNIT NO. 2

19 effective full power years (EFPY) of operation at the vessel I. D. and 32 EFPY (design life) at the vessel 1/4 T position. This projection will be refined as additional surveillance capsules are removed.

A similar approach can be taken to estimate the increase in RT_{NDT} as a function of reactor power generation. Again, a method for estimating shifts in RT_{NDT} is given in Regulatory Guide 1.99, Revision 1. Figure 9 compares the Indian Point Unit No. 2 surveillance data on the three plate materials to selected portions of Figure 1 of Regulatory Guide 1.99, Revision 1. The results indicate that the measured shifts in RT_{NDT} are higher than predicted by Regulatory Guide 1.99, Revision 1.

The predicted shifts in RT_{NDT} for the Indian Point Unit No. 2 reactor pressure vessel obtained from Figure 9 are summarized in Table XI. The values predicted at the 1/4 T and 3/4 T after 5 EFPY are used to develop heatup and cooldown limit curves to meet the requirements of Appendix G to Section III of the ASME Code.

These projections for C_v shelf energy reductions and RT_{NDT} shifts are based on one data point each for the three vessel plates but, more importantly, no data on the weld metal. Even if it is assumed that the weld metal is more sensitive than Plate B2002-3 to radiation embrittlement, it will require a number of years of operation for the weld metal to become controlling because the initial RT_{NDT} of the weld metal is -80°F[13], nearly 100°F below that of Plate B2002-3.

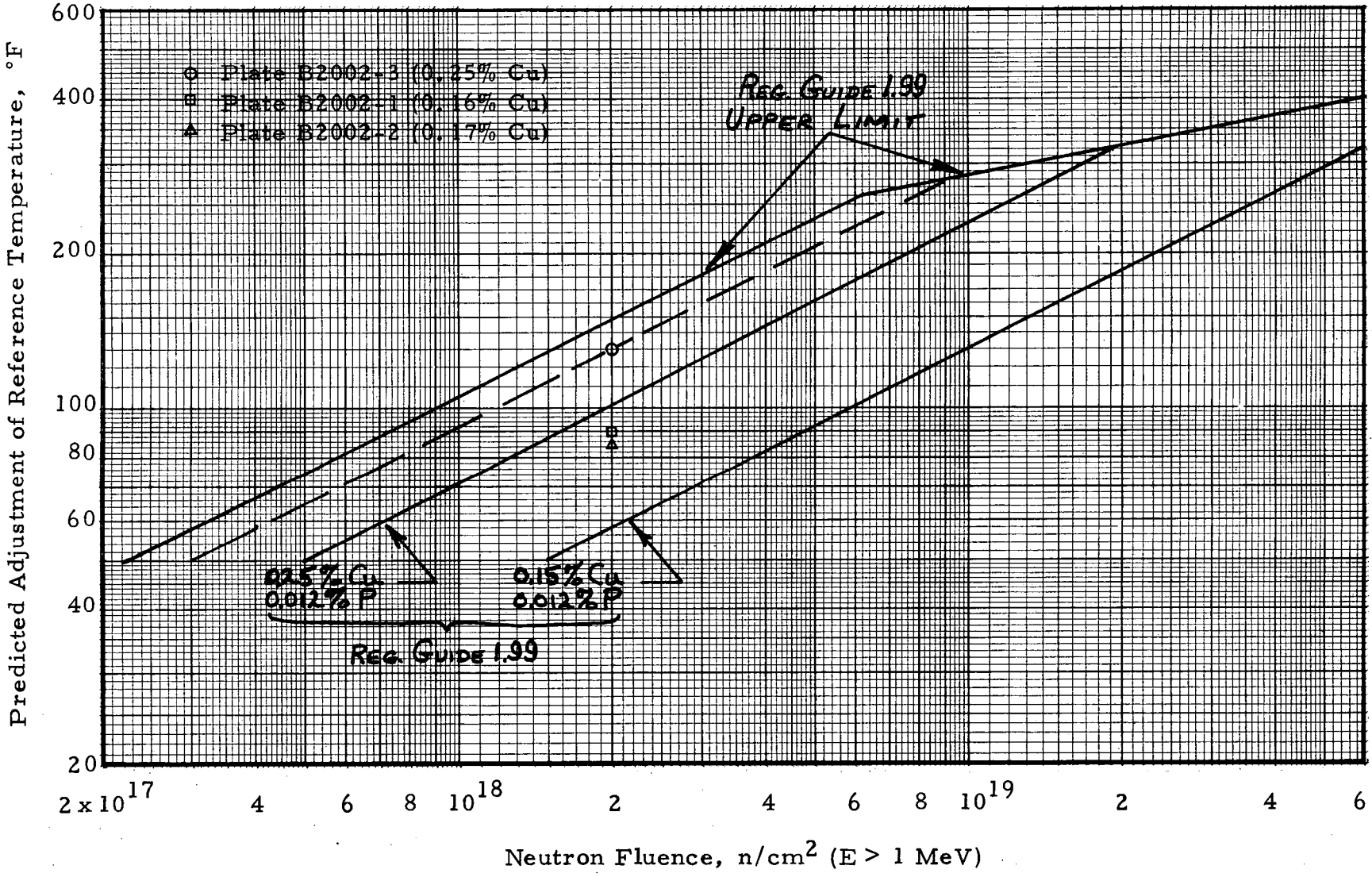

FIGURE 9. EFFECT OF NEUTRON FLUENCE ON RT_{NDT} SHIFT, INDIAN POINT UNIT NO. 2

TABLE XI

Projected Shifts in RT_{NDT} for Indian Point Unit No. 2

Location	5 EFPY[a]		32 EFPY	
	Fluence[b]	ΔRT_{NDT}[c]	Fluence	ΔRT_{NDT}
Pressure Vessel I. D.	2.5×10^{18}	145 °F	1.6×10^{19}	310°F
Pressure Vessel 1/4 T	1.5×10^{18}	110 °F	9.6×10^{18}	280°F
Pressure Vessel 3/4 T	3.7×10^{17}	50 °F	2.4×10^{18}	140°F

(a) 1 EFPY = 1,006,700 MWD_t
(b) Neutrons/cm^2, E > 1 MeV
(c) ΔRT_{NDT} is maximum for Plate B2002-3. Refer to Figure 9.

It is anticipated that the reliability of the trend curves will be improved as more surveillance data becomes available and a better understanding of the factors affecting radiation embrittlement has been achieved. As an example of the latter, Mr. E. C. Biemiller of Combustion Engineering, in a paper given at the ASTM E 10 Symposium on Effects of Radiation on Structural Materials in St. Louis, May 4-6, 1976, indicated that a parameter of (% Ni + % Si) ÷ (% Mo + % Cr + % Mn) may explain the variation in radiation embrittlement observed in ferritic materials of nominally the same copper content. Also, the Metal Properties Council is developing new radiation damage curves that will be based on more data than those currently in use.

The Indian Point Unit No. 2 reactor vessel surveillance program schedule proposed by Westinghouse[13] is summarized in Table XII. It has been organized to satisfy Appendix H of 10CFR50 as closely as possible. There are seven additional capsules in the vessel, three of which contain weld metal specimens. There is no reason to consider changing the basic concept of the removal schedule until a capsule containing weld metal has been removed and tested. However, consideration may be given to the removal of Capsule Y instead of Capsule S at the time of the second region replacement because Capsule Y contains Charpy V-notch specimens from Plate B2002-3 and Capsule S does not.

TABLE XII

Proposed Reactor Vessel Surveillance Capsule Schedule
Indian Point Unit No. 2

Capsule Ident.	Capsule Type[a]	Material Content[b]	Exposure Time
S	II	1, W, H	Second Region Replacement
T	I	1, 2, 3	Removed 1976
U	I	1, 2, 3	Spare
V	II	2, W, H	10 Years
W	I	1, 2, 3	Spare
X	I	1, 2, 3	Spare
Y	II	3, W, H	Spare
Z	I	1, 2, 3	Fourth Region Replacement

(a) Type I contains all three vessel plates. Type II contains weld metal, HAZ and one vessel plate.

(b) Material Code:
1 - Plate B2002-1; 2 - Plate B2002-2; 3 - Plate B2002-3;
W - Weld Metal; H - HAZ

VI. HEATUP AND COOLDOWN LIMIT CURVES FOR NORMAL OPERATION OF INDIAN POINT UNIT NO. 2

Indian Point Unit No. 2 is a 2758 Mw_t pressurized water reactor operated by Consolidated Edison Company. The unit has been provided with a reactor vessel material surveillance program as required by 10CFR50, Appendix H.

The first surveillance capsule (Capsule T) was removed during the 1976 refuelling outage. This capsule was tested by Southwest Research Institute, the results being described in the earlier sections of this report. In summary, these results indicate that:

(1) The RT_{NDT} of the plate materials in Capsule T increased a maximum of 140 °F as a result of exposure to a neutron fluence of 2.02×10^{18} neutrons/cm^2 ($E > 1$ MeV).

(2) Based on a ratio of 2.9 between the fast neutron flux at the Capsule T location and the maximum incident on the vessel wall, the vessel wall fluence was 6.97×10^{17} neutrons/cm^2 ($E > 1$ MeV) at the time of removal of Capsule T.

(3) The maximum shift in RT_{NDT} after 5 effective full power years (EFPY) of operation was predicted to be 105 °F at the 1/4 T and 50 °F at the 3/4 T vessel wall locations, as controlled by Plate B2002-3. After 32 EFPY, the corresponding values are predicted to be 270 °F and 130 °F, respectively.

The Unit No. 2 heatup and cooldown limit curves for 5 EFPY have been computed on the basis of the RT_{NDT} of Plate B2002-3 because it is anticipated that the RT_{NDT} of reactor vessel beltline material will be highest for Plate B2002-3 at least through that time period. The procedures employed by SwRI are described in Appendix B.

The values of RT_{NDT} for the beltline regions of Indian Point Unit No. 2 were derived from (1) the surveillance program test results, (2) ratios of fast flux at the capsule location to the maximum fast flux at the 1/4T and 3/4T locations in the vessel wall, (3) Regulatory Guide 1.99, Revision 1, trend curves of increase in RT_{NDT} as a function of neutron fluence ($E > 1$ MeV), and (4) the initial RT_{NDT} of the primary system materials.

The initial value of RT_{NDT} for the Indian Point Unit No. 2 vessel was reported to be 60°F based on Plates B2002-1 and B2002-3.[21] As Plate B2002-3 had the highest initial Charpy V-notch transition temperature[13] and the greatest radiation-induced shift in transition temperature, the unirradiated and irradiated data for that material were reduced by 35% and replotted in Figure 10 to confirm the shift in RT_{NDT} caused by the Capsule T irradiation. The unirradiated RT_{NDT} (defined as 60°F less than the 50 ft-lb Charpy V-notch temperature) would then be 50°F. However, the 60°F figure given in the Indian Point Unit No. 2 Technical Specifications was used as the initial RT_{NDT} in this analysis.

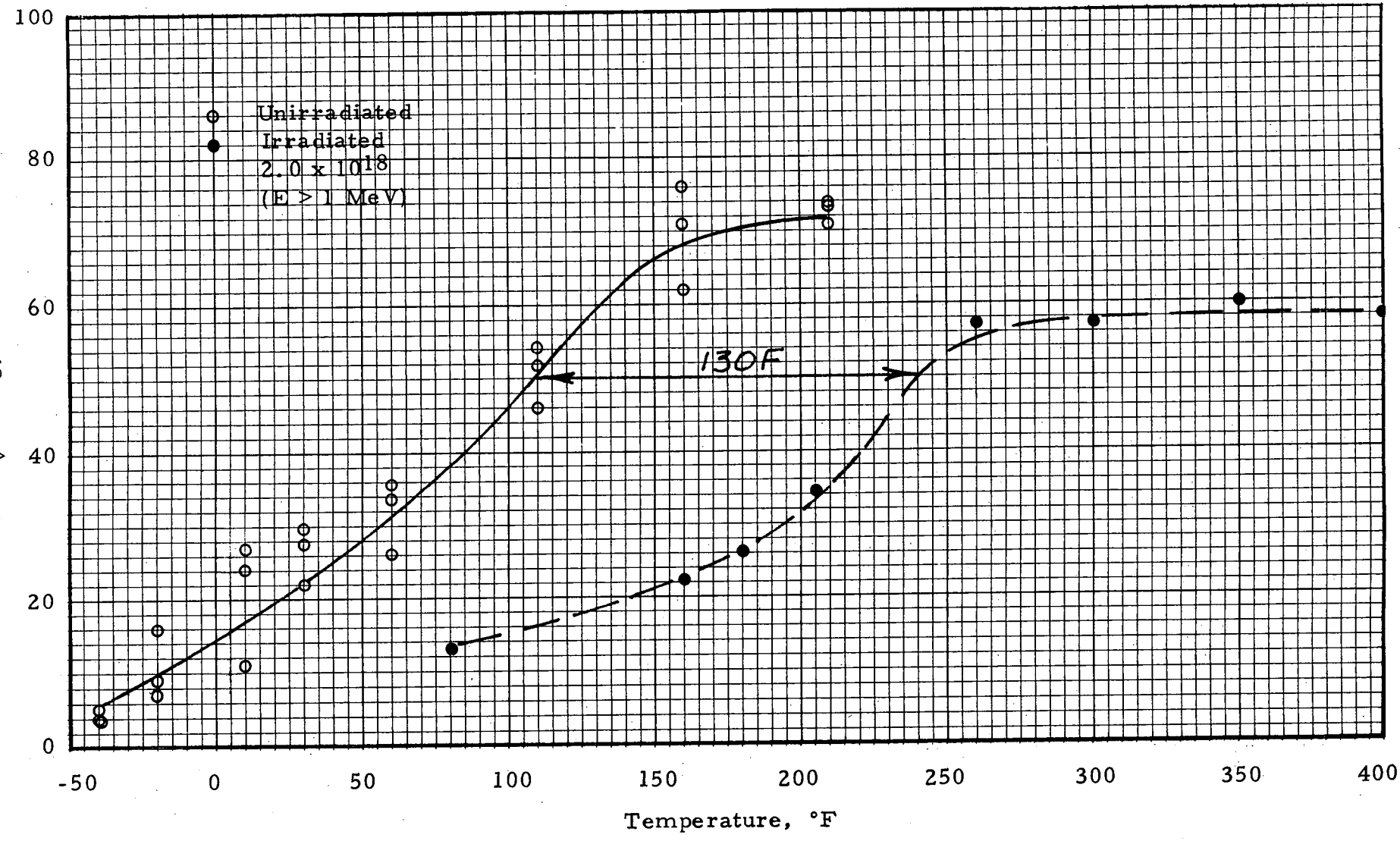

FIGURE 10. ESTIMATED TRANSVERSE CHARPY V-NOTCH PROPERTIES OF PLATE B2002-3

The following pressure vessel constants were employed as input data in this analysis:

Vessel Inner Radius, r_i	=	86.50 in.
Vessel Outer Radius, r_o	=	95.34 in.
Operating Pressure, P_o	=	2235 psig
Initial Temperature, T_o	=	70°F
Final Temperature, T_f	=	550°F
Effective Coolant Flow Rate, Q	=	136.3×10^6 lb_m/hr
Effective Flow Area, A	=	26.719 ft^2
Effective Hydraulic Diameter, D	=	15.051 in.

Heatup curves were computed for a heatup rate of 60°F/hr. Since lower rates tend to raise the curve in the central region (see Appendix B), these curves apply to all heating rates up to 60°F/hr. Cooldown curves were computed for cooldown rates of 0°F/hr (steady state), 20°F/hr, 60°F/hr, and 100°F/hr. The 20°F/hr curve would apply to cooldown rates up to 20°F/hr; the 60°F/hr curve would apply to rates from 20°F to 60°F/hr; the 100°F/hr curve would apply to rates from 60°F/hr to 100°F/hr.

The Unit No. 2 heatup and cooldown curves for up to 5 EFPY are given in Figures 11, 12 and 13.

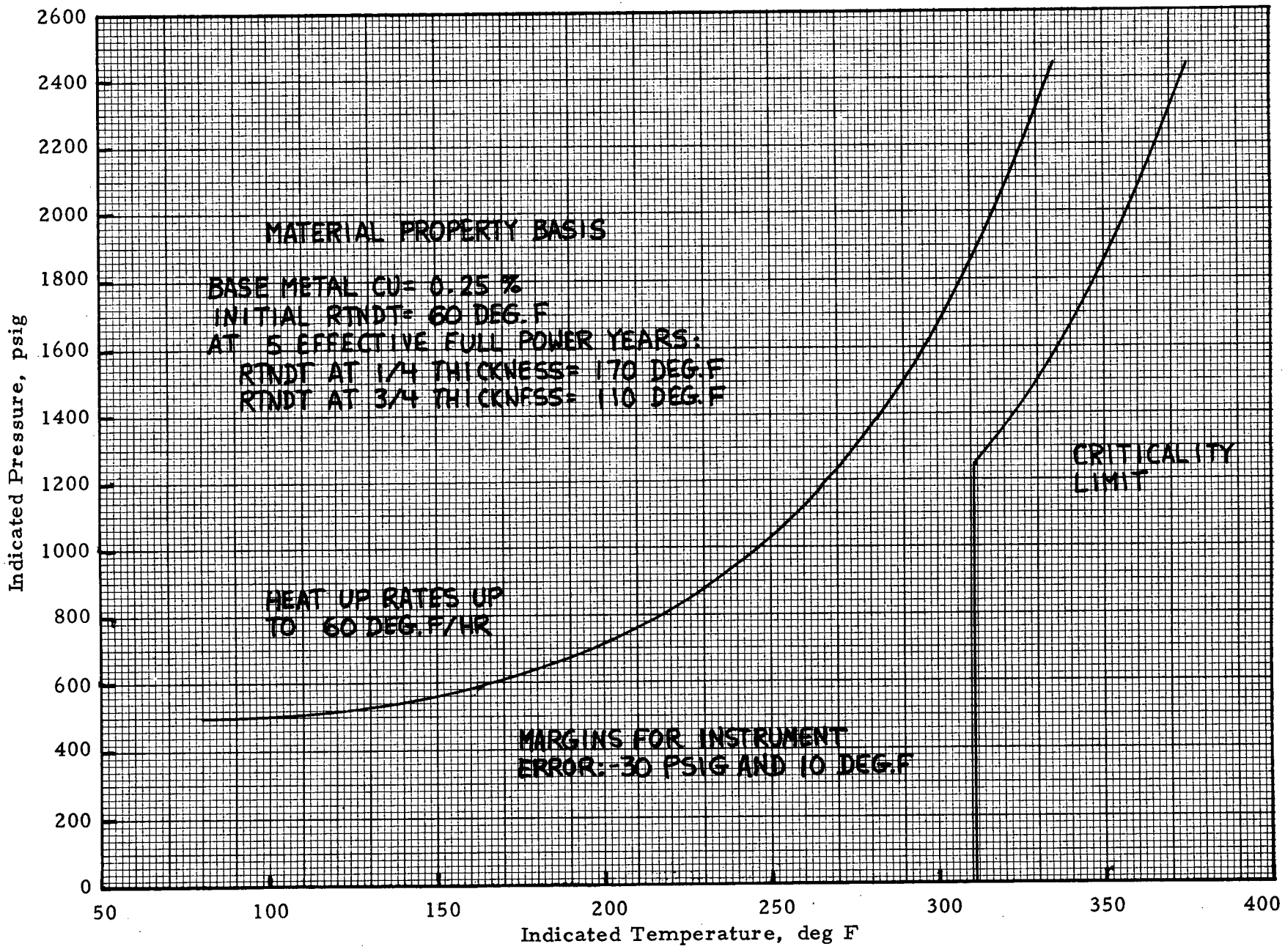

FIGURE 11. INDIAN POINT UNIT NO. 2 REACTOR COOLANT HEATUP LIMITATIONS APPLICABLE FOR PERIODS UP TO 5 EFFECTIVE FULL POWER YEARS

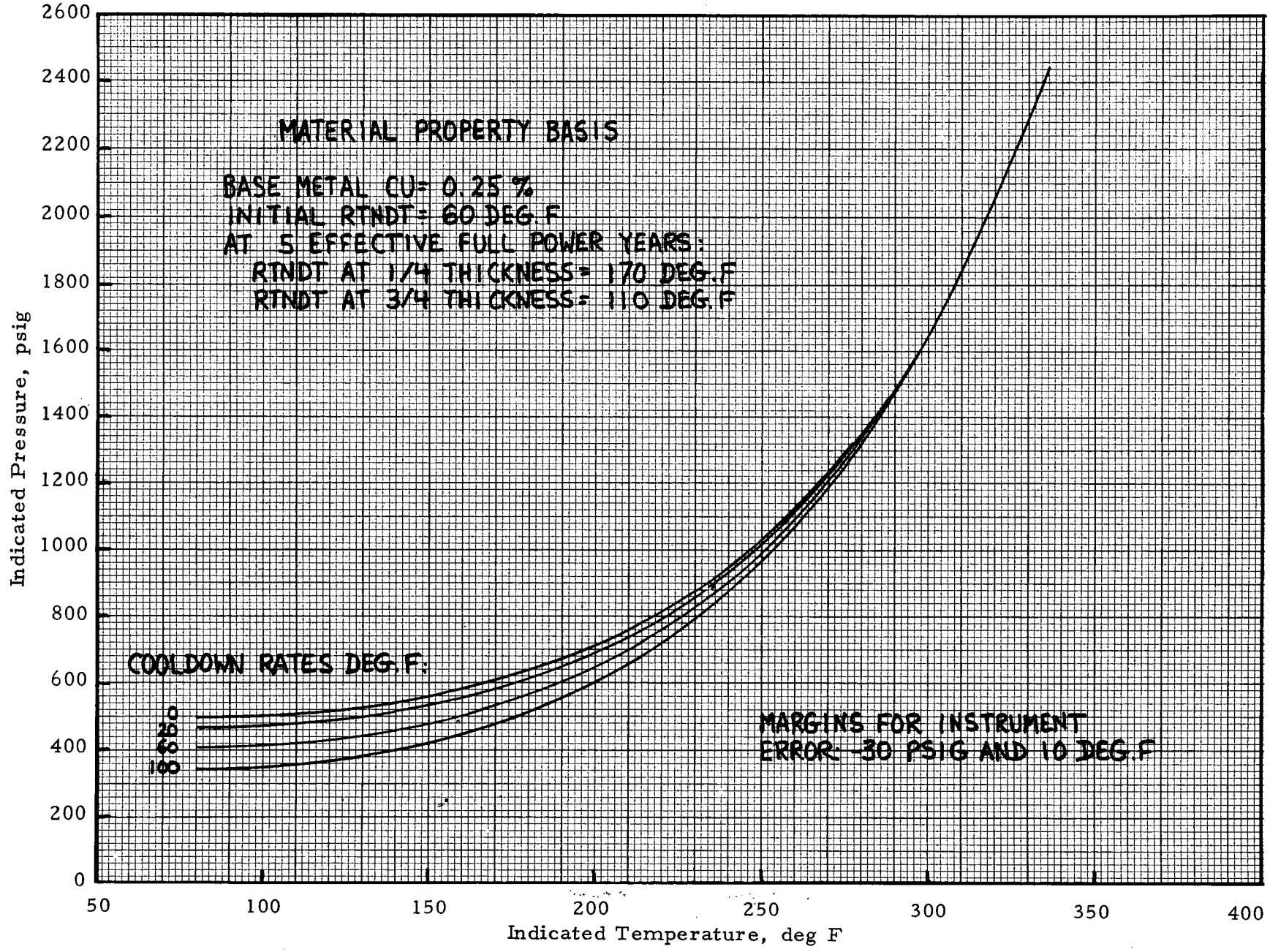

FIGURE 12. INDIAN POINT UNIT NO. 2 REACTOR COOLANT COOLDOWN LIMITATIONS APPLICABLE FOR PERIODS UP TO 5 EFFECTIVE FULL POWER YEARS

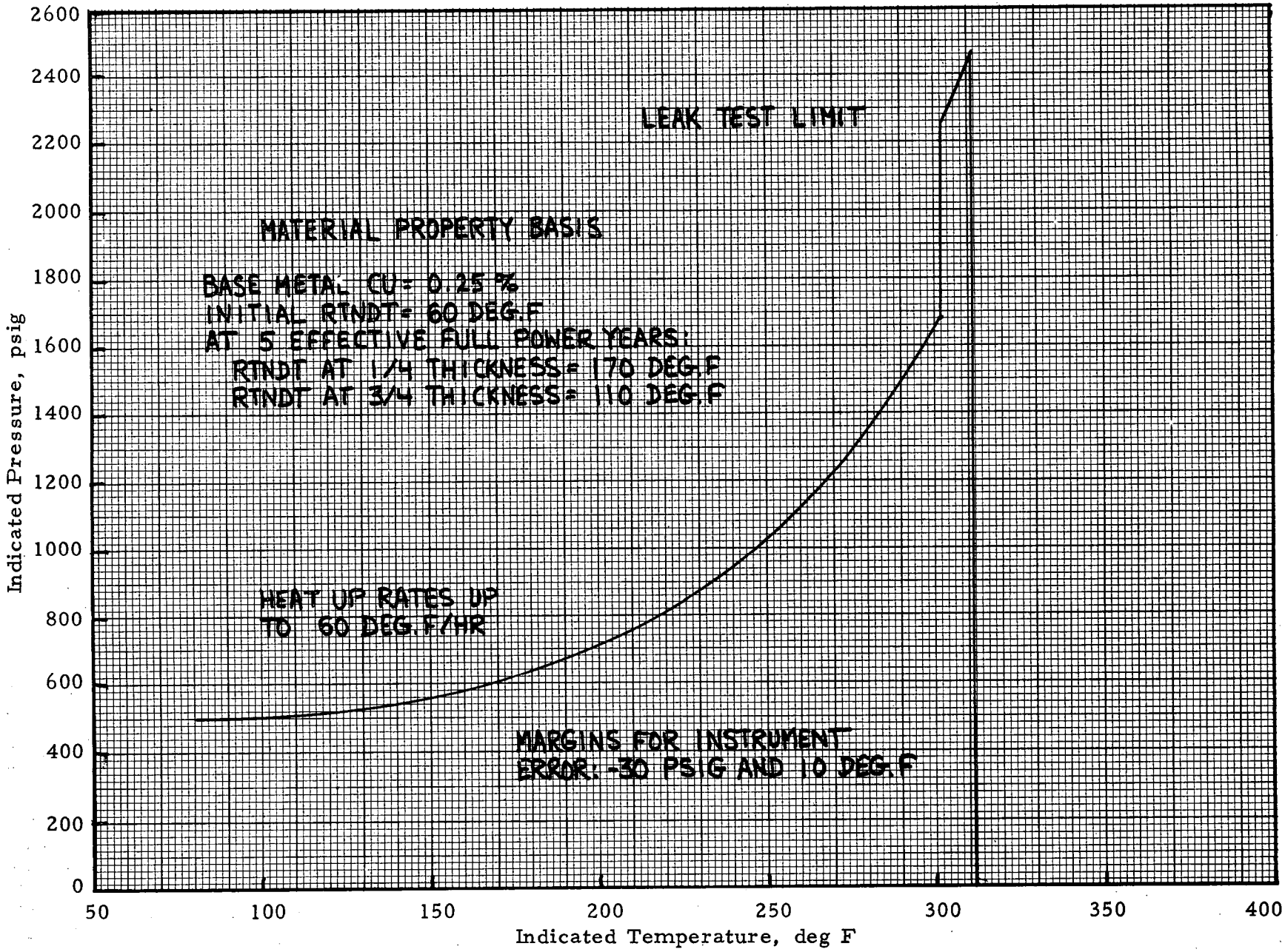

FIGURE 13. INDIAN POINT UNIT NO. 2 INSERVICE LEAK TEST LIMITATIONS APPLICABLE FOR PERIODS UP TO 5 EFFECTIVE FULL POWER YEARS

VII. REFERENCES

1. Title 10, Code of Federal Regulations, Part 50, "Licensing of Production and Utilization Facilities."

2. ASME Boiler and Pressure Vessel Code, Section III, "Nuclear Power Plant Components," 1974 Edition.

3. ASTM E 208-69, "Standard Method for Conducting Drop-Weight Test to Determine Nil-Ductility Transition Temperature of Ferritic Steels," 1975 Annual Book of ASTM Standards.

4. Steele, L. E., and Serpan, C. Z., Jr., "Analysis of Reactor Vessel Radiation Effects Surveillance Programs," ASTM STP 481, December 1970.

5. Steele, L. E., "Neutron Irradiation Embrittlement of Reactor Pressure Vessel Steels," International Atomic Energy Agency, Technical Reports Series No. 163, 1975.

6. ASME Boiler and Pressure Vessel Code, Section XI, "Rules for Inservice Inspection of Nuclear Power Plant Components," 1974 Edition.

7. Regulatory Guide 1.99, Revision 1, Office of Standards Development, U.S. Nuclear Regulatory Commission, April 1977.

8. Comments on Regulatory Guide 1.99, Westinghouse Electric Corporation, Obtained from NRC Public Document Room, Washington, D.C.

9. Position on Regulatory Guide 1.99, Combustion Engineering Power Systems, Obtained from NRC Public Document Room, Washington, D.C.

10. ASTM E 185-73, "Standard Recommended Practice for Surveillance Tests for Nuclear Reactor Vessels," 1975 Annual Book of ASTM Standards.

11. ASTM E 399-74, "Standard Method of Test for Plane-Strain Fracture Toughness of Metallic Materials," 1975 Annual Book of ASTM Standards.

12. Witt, F. J., and Mager, T. R., "A Procedure for Determining Bounding Values of Fracture Toughness K_{Ic} at Any Temperature," ORNL-TM-3894, October 1972.

13. "Indian Point Unit No. 2 Reactor Vessel Radiation Surveillance Program," WCAP-7323, May 1969.

14. "Indian Point Unit No. 3 Reactor Vessel Radiation Surveillance Program," WCAP-8475, January 1975.

15. Letter, Westinghouse to Con Edison, May 16, 1975.

16. ENDF/B-IV, Dosimetry Tape 412, Mat No. 6417 (26-Fe-54), July 1974.

17. ASTM E 322, "Standard Method for Spectrochemical Analysis of Low Alloy Steels and Cast Irons Using an X-ray Fluorescence Spectrometer," 1974 Annual Book of ASTM Standards.

18. Loss, F. J., Hawthorne, J. R., Serpan, C. Z., Jr., and Puzak, P. P., "Analysis of Radiation-Induced Embrittlement Gradients on Fracture Characteristics of Thick-Walled Pressure Vessel Steels," NRL Report 7209, March 1, 1971.

19. Telecon, E. B. Norris to Ken Hogue (NRC Staff) January 19, 1977.

20. Hazleton, W. S., Anderson, S. L., and Yanichko, S. E., "Basis for Heatup and Cooldown Limit Curves," WCAP-7924, July 1972.

21. Indian Point Unit No. 2 Technical Specifications, Amendment No. 28, dated April 26, 1976.

APPENDIX A

TENSILE TEST RECORDS

Southwest Research Institute
Department of Materials Engineering

TENSILE TEST DATA SHEET

Test No. T- 2 | Est. U. T. S. _____ psi | Project No. 2453

Spec. No. 1-1 | Initial G. L. 1.0 in. | Machine No. Ollen

Temp. 550 °F | Initial Dia. .252 in. | Date 6/28/76

Strain Rate .01 in/in/min | Initial Thickness _____ in. | Initial Area .0499

Initial Width _____ in.

Top Temp. 550 °F | Maximum Load 4800 lb.

Bottom Temp. 549 °F | 0.2% Offset Load 3550 lb.

Final G. L. 1.322 in. | 0.2% Offset Load _____ lb.

Final Dia. .168 in. | Upper Yield Point _____ lb.

Final Area .0222 in.^{2}

$$\text{U. T. S.} = \frac{\text{Maximum Load}}{\text{Initial Area}} = \frac{4800}{.0499} = 96,200 \text{ psi}$$

$$\text{0.2\% Y. S.} = \frac{\text{0.2\% Offset Load}}{\text{Initial Area}} = \frac{3550}{.0499} = 71,100 \text{ psi}$$

$$\text{0.2\% Y. S.} = \frac{\text{0.2\% Offset Load}}{\text{Initial Area}} = \text{_____ psi}$$

$$\text{Upper Y. S.} = \frac{\text{Upper Yield Point}}{\text{Initial Area}} = \text{_____ psi}$$

$$\text{\% Elongation} = \frac{\text{Final G. L.} - \text{Initial G. L.}}{\text{Initial G. L.}} \times 100 = \frac{1.322 - 1.0}{1.0} \times 100 = 20.4 \%$$

$$\text{\% R.A.} = \frac{\text{Initial Area} - \text{Final Area}}{\text{Initial Area}} \times 100 = \frac{.0499 - .0222}{.0499} \times 100 = 55.5 \%$$

GBJ Hess R. L. Ollen

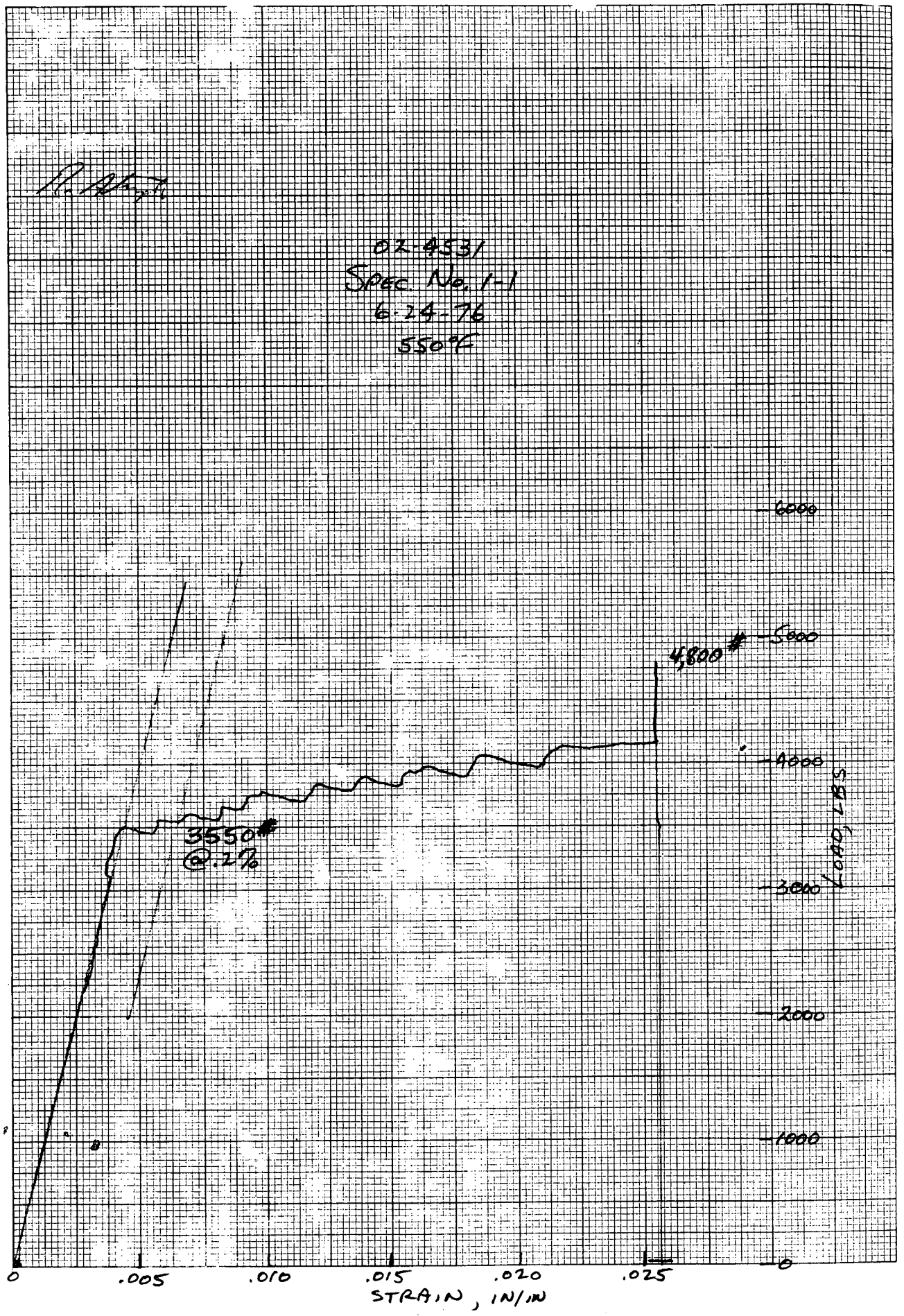

Southwest Research Institute
Department of Materials Engineering

TENSILE TEST DATA SHEET

Test No. T- 3 | Est. U.T.S. _____ psi | Project No. 02-4531

Spec. No. 2-1 | Initial G.L. 1.00 in. | Machine No. DILLON

Temp. +550°F °F | Initial Dia. .201 in. | Date 6-24-76

Strain Rate .01 in/min | Initial Thickness _____ in. | Initial Area .0495

Initial Width _____ in.

Top Temp. +550° °F | Maximum Load 4,250 lb.

Bottom Temp. +550° °F | 0.2% Offset Load 2900 lb.

Final G.L. 1.207 in. | 0.2% Offset Load _____ lb.

Final Dia. .149 in. | Upper Yield Point _____ lb.

Final Area .0174 in.^{2}

$$\text{U.T.S.} = \frac{\text{Maximum Load}}{\text{Initial Area}} = 85,900 \text{ psi}$$

$$\text{0.2\% Y.S.} = \frac{\text{0.2\% Offset Load}}{\text{Initial Area}} = 58,600 \text{ psi}$$

$$\text{0.2\% Y.S.} = \frac{\text{0.2\% Offset Load}}{\text{Initial Area}} = \text{_____ psi}$$

$$\text{Upper Y.S.} = \frac{\text{Upper Yield Point}}{\text{Initial Area}} = \text{_____ psi}$$

$$\text{\% Elongation} = \frac{\text{Final G.L. - Initial G.L.}}{\text{Initial G.L.}} \times 100 = 20.7 \%$$

$$\text{\% R.A.} = \frac{\text{Initial Area - Final Area}}{\text{Initial Area}} \times 100 = 64.8 \%$$

E. B. Norris — Richard C. Stroh

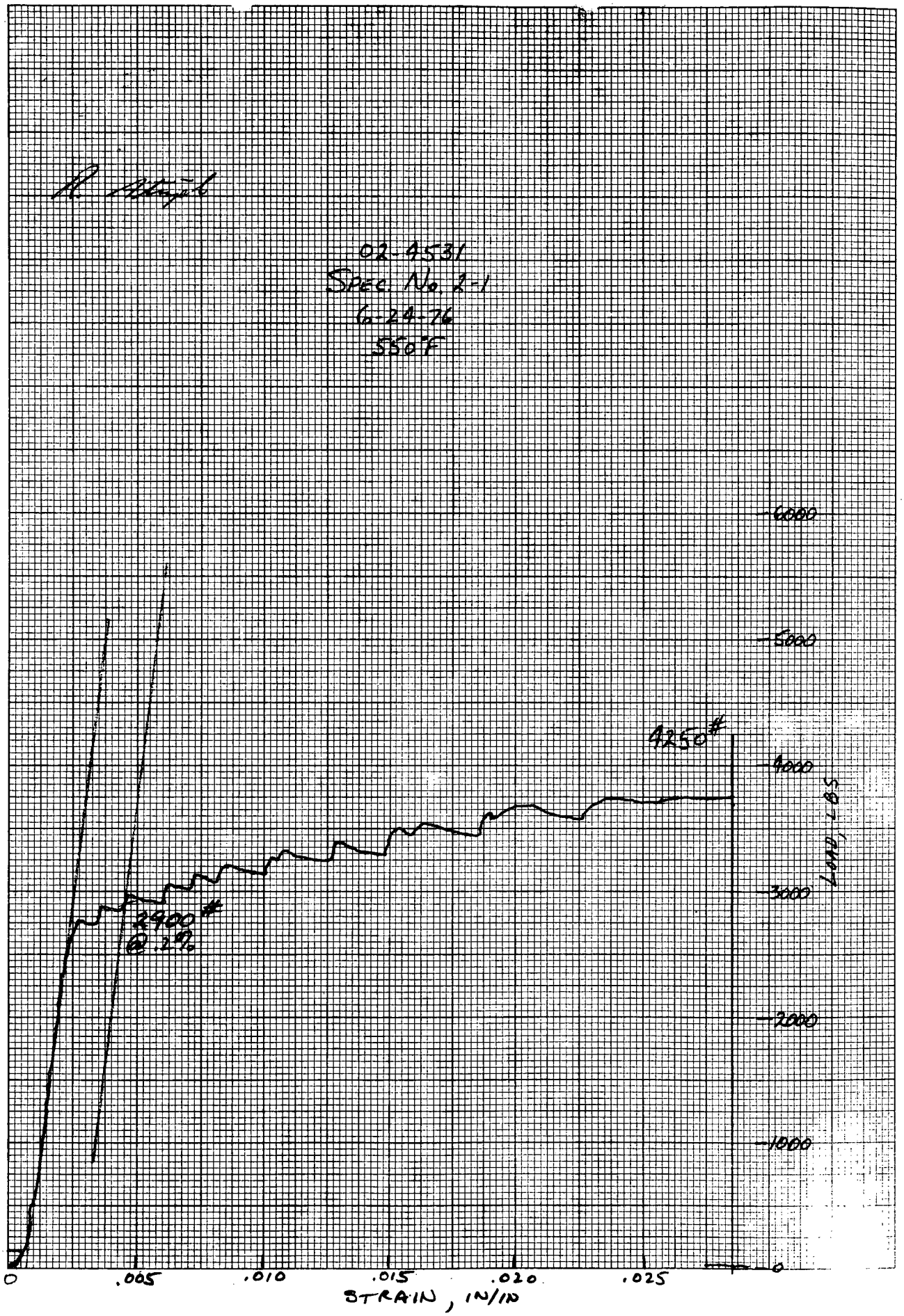

Southwest Research Institute
Department of Materials Engineering

TENSILE TEST DATA SHEET

Test No. T- 1 | Est. U.T.S. _____ psi | Project No. 02-4531

Spec. No. 3-1 | Initial G.L. 1.000 in. | Machine No. DILLON

Temp. 550° °F | Initial Dia. .250 in. | Date 6-23-76

Strain Rate .01 in/in/min | Initial Thickness _____ in. | Initial Area .0491

Initial Width _____ in.

Top Temp. 550° °F | Maximum Load 4390 lb.

Bottom Temp. 551° °F | 0.2% Offset Load 3100 lb.

Final G.L. 1.202 in. | 0.2% Offset Load _____ lb.

Final Dia. .152 in. | Upper Yield Point _____ lb.

Final Area .0181 in.^{2}

$$\text{U.T.S.} = \frac{\text{Maximum Load}}{\text{Initial Area}} = \frac{4390}{.0491} = 89,400 \text{ psi}$$

$$\text{0.2\% Y.S.} = \frac{\text{0.2\% Offset Load}}{\text{Initial Area}} = \frac{3100}{.0491} = 63,100 \text{ psi}$$

$$\text{0.2\% Y.S.} = \frac{\text{0.2\% Offset Load}}{\text{Initial Area}} = \text{_____ psi}$$

$$\text{Upper Y.S.} = \frac{\text{Upper Yield Point}}{\text{Initial Area}} = \text{_____ psi}$$

$$\text{\% Elongation} = \frac{\text{Final G.L. - Initial G.L.}}{\text{Initial G.L.}} \times 100 = \frac{.202}{1.000} \times 100 = 20.2 \%$$

$$\text{\% R.A.} = \frac{\text{Initial Area - Final Area}}{\text{Initial Area}} \times 100 = \frac{.0491 - .0181}{.0491} \times 100 = 63.1 \%$$

Checked 7/1/76 B.M. Mott Richard E. Ott

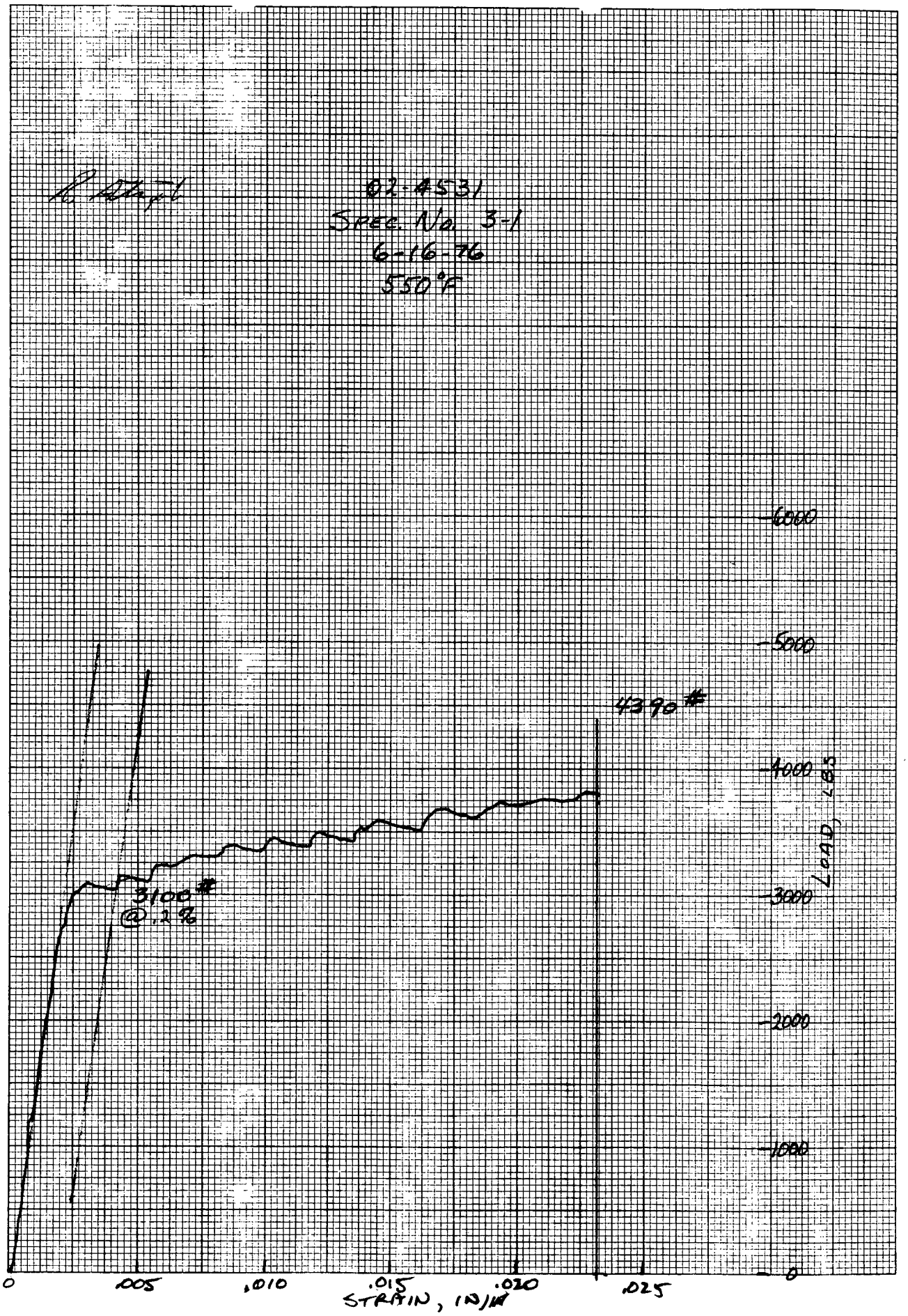

APPENDIX B

PROCEDURE FOR THE GENERATION OF ALLOWABLE PRESSURE-TEMPERATURE LIMIT CURVES FOR NUCLEAR POWER PLANT REACTOR VESSELS

PROCEDURE FOR THE GENERATION OF ALLOWABLE PRESSURE-TEMPERATURE LIMIT CURVES FOR NUCLEAR POWER PLANT REACTOR VESSELS

A. Introduction

The following is a description of the basis for the generation of pressure-temperature limit curves for inservice leak and hydrostatic tests, heatup and cooldown operations, and core operation of reactor pressure vessels. The safety margins employed in these procedures equal or exceed those recommended in the ASME Boiler and Pressure Vessel Code, Section III, Appendix G, "Protection Against Nonductile Failure."

B. Background

The basic parameter used to determine safe vessel operational conditions is the stress intensity factor, K_I, which is a function of the stress state and flaw configuration. The K_I corresponding to membrane tension is given by

$$K_{Im} = M_m \cdot \sigma_m \tag{1}$$

where M_m is the membrane stress correction factor for the postulated flaw and σ_m the membrane stress. Likewise, K_I corresponding to bending is given by

$$K_{Ib} = M_b \cdot \sigma_b \tag{2}$$

where M_b is the bending stress correction factor and σ_b is the bending stress. For vessel section thickness of 4 to 12 inches, the maximum

postulated surface flaw, which is assumed to be normal to the direction of maximum stress, has a depth of 0.25 of the section thickness and a length of 1.50 times the section thickness. Curves for M_m versus the square root of the vessel wall thickness for the postulated flaw are given in Figure 1 as taken from the Pressure Vessel Code (ref. Figure G-2114.1). These curves are a function of the stress ratio parameter σ/σ_y, where σ_y is the material yield strength which is taken to be 50,000 psi. The bending correction factor is defined as 2/3 M_m and is therefore determined from Figure 1 as well. The basis for these curves is given in ASME Boiler and Pressure Vessel Code, Section XI, "Rules for Inservice Inspection of Nuclear Power Plant Components," Article A-3000.

The Code specifies the minimum K_I that can cause failure as a function of material temperature, T, and its reference nil ductility temperature, RT_{NDT}. This minimum K_I is defined as the reference stress intensity factor, K_{IR}, and is given by

$$K_{IR} = 26777. + 1223. \exp\left[0.014493(T - RT_{NDT} + 160)\right] \qquad (3)$$

where all temperatures are in degrees Fahrenheit. A plot of this expression is given in Figure 2 taken from the Code (ref. Figure G-2010.1).

C. Pressure-Temperature Relationships

1. Inservice Leak and Hydrostatic Test

During performance of inservice leak and hydrostatic tests, the reference stress intensity factor, K_{IR}, must always be greater than

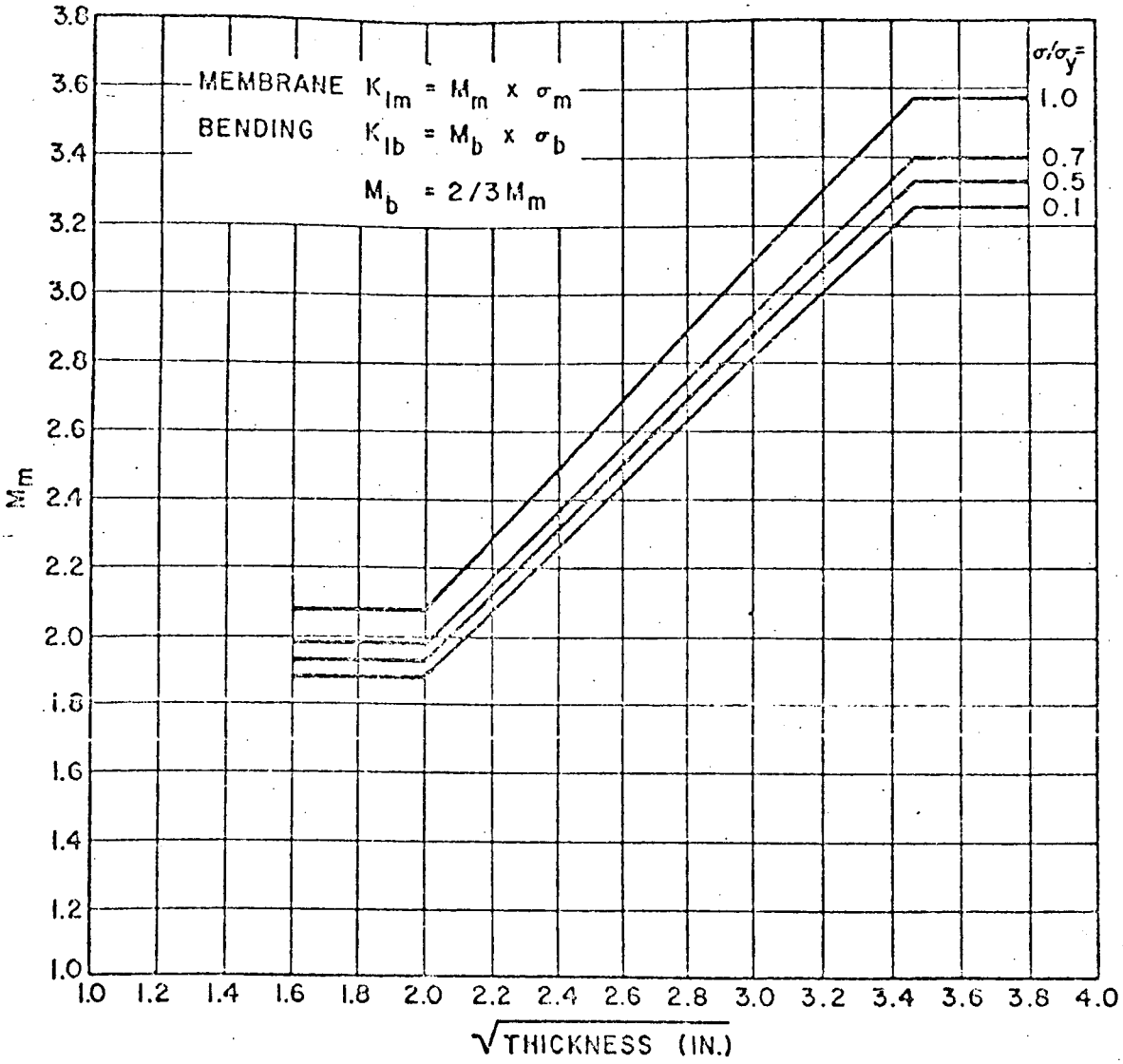

FIGURE 1. STRESS CORRECTION FACTOR

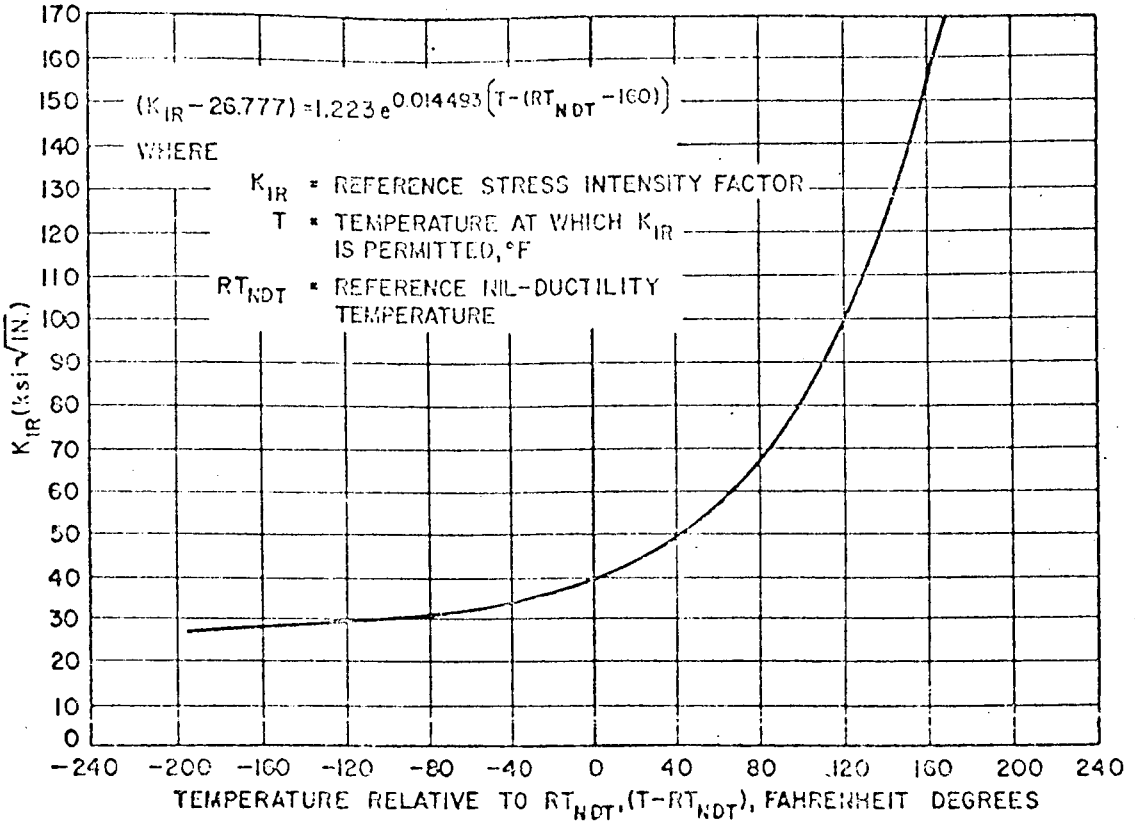

FIGURE 2. REFERENCE STRESS INTENSITY FACTOR

1.5 times the K_I caused by pressure, thus

$$1.5\ K_{Ip} < K_{IR} \tag{4}$$

or

$$1.5\ M_m\ \sigma_m < K_{IR}\,. \tag{5}$$

For a cylinder with inner radius r_i and outer radius r_o, the stress distribution due to internal pressure is given by

$$\sigma(r) = \left(\frac{r_i^2}{r_o^2 - r_i^2}\right)\left(\frac{r_o^2 + r^2}{r^2}\right)\,. \tag{6}$$

With 1/4T flaws possible at both inner and outer radial locations, i.e., at $r_{1/4} = r_i + 1/4(r_o - r_i)$ and $r_{3/4} = r_i + 3/4(r_o - r_i)$, the maximum stress will occur at the inner flaw location, thus

$$\sigma_{max} = P_o\left(\frac{r_i^2}{r_o^2 - r_i^2}\right)\left[\frac{r_o^2 + (1/4r_o + 3/4r_i)^2}{(1/4r_o + 3/4r_i)^2}\right]\,. \tag{7}$$

With the operation pressure known, i.e., P_o, we determine the minimum coolant temperature that will satisfy Equation (4) by evaluating

$$K_{IR} = 1.5\ M_m\ \sigma_{max} \tag{8}$$

and determine the corresponding coolant temperature, T, from Equation (3) for the given RT_{NDT} at the 1/4T location. For this calculation, Equation (3) takes the form

$$T = RT_{NDT}(1/4T) - 160. + 68.9988\ \ln\left[\frac{K_{IR} - 26777.}{1223.}\right]\,. \tag{9}$$

The inservice curves are generated for an operating pressure range of .96 P_o to 1.14 P_o, where P_o is the design operating pressure.

2. Heatup and Cooldown Operations

At all times during heatup and cooldown operations, the reference stress intensity factor, K_{IR}, must always be greater than the sum of 2 times the K_{Ip} caused by pressure and the K_{It} caused by thermal gradients, thus

$$2.0\ K_{Ip} + 1.0\ K_{It} < K_{IR} \tag{10}$$

or

$$2.0\ M_m\ \sigma_{max} = K_{IR} - K_{It} \tag{11}$$

where σ_{max} is the maximum allowable stress due to internal pressure, and K_{It} is the equivalent linear stress intensity factor produced by the thermal gradients. To obtain the equivalent linear stress intensity factor due to thermal gradients requires a detailed thermal stress analysis. The details of the required analysis are given in Section D.

During heatup the radial stress distributions due to internal pressure and thermal gradients are shown schematically in Figure 3a. Assuming a possible flaw at the 1/4T location, we see from Figure 3a that the thermal stress tends to alleviate the pressure stress at this point in the vessel wall and, therefore, the steady state pressure stress would represent the maximum stress condition at the 1/4T location. At

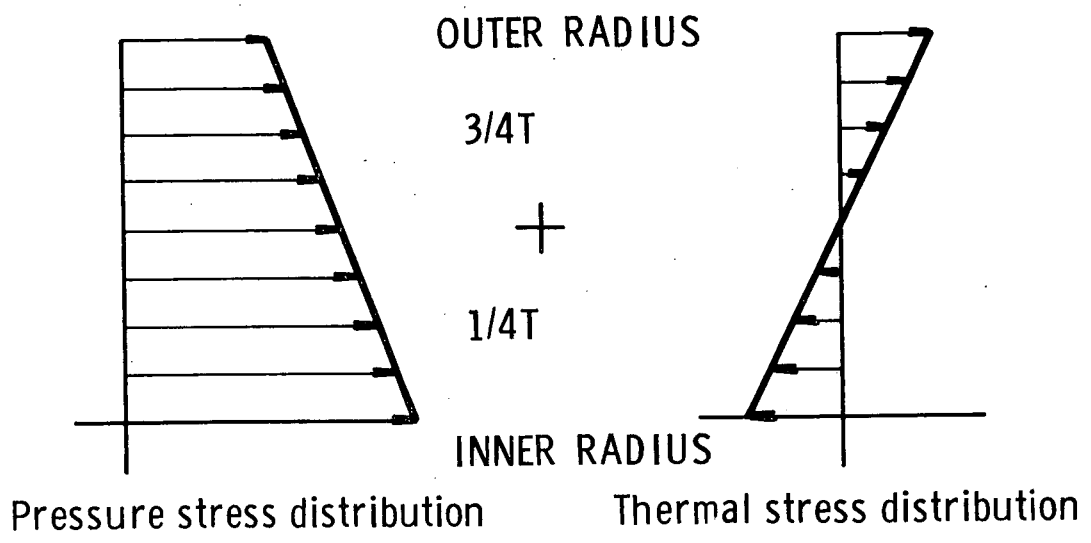

(a) Heatup

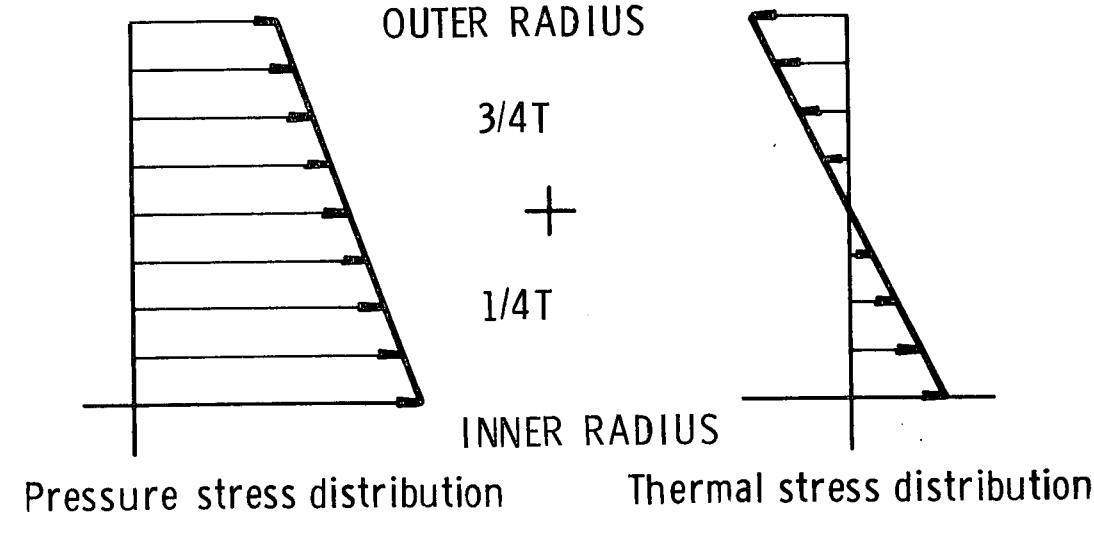

(b) Cooldown

Figure 3. Heatup and Cooldown Stress Distribution

the 3/4T flaw location, the pressure stress and thermal stress add and, therefore, the combination for a given heatup rate represents the maximum stress at the 3/4T location. The maximum overall stress between the 1/4T and 3/4T location then determines the maximum allowable reactor pressure at the given coolant temperature.

The heatup pressure-temperature curves are thus generated by calculating the maximum steady state pressure based on a possible flaw at the 1/4T location from

$$P_{max}(1/4T) = \frac{K_{IR}}{2M_m\left(\frac{r_i^2}{r_o^2 - r_i^2}\right)\left(\frac{r_o^2 + (1/4r_o + 3/4r_i)^2}{(1/4r_o + 3/4r_i)^2}\right)} \qquad (12)$$

where M_m is determined from the curves in Figure 1 and K_{IR} is obtained from Equation (3) using the coolant temperature and RT_{NDT} at the 1/4T location. Here we may note that M_m must be iterated for since it is a function of the final stress ratio to yield strength (σ/σ_y).

At the 3/4T location, the maximum pressure is determined from Equation (11) as

$$P_{max}(3/4T) = \frac{K_{IR} - K_{It}}{2M_m\left(\frac{r_i^2}{r_o^2 - r_i^2}\right)\left(\frac{r_o^2 + (1/4r_i + 3/4r_o)^2}{(1/4r_i + 3/4r_o)^2}\right)} \qquad (13)$$

where K_{IR} is obtained from Equation (2) using the material temperature and RT_{NDT} at the 3/4T location and K_{It} is determined from the analysis procedure outlined in Section D. M_m is determined from Figure 1.

The minimum of these maximum allowable pressures at the given coolant temperature determines the maximum operation pressure. Each heatup rate of interest must be analyzed on an individual basis.

The cooldown analysis proceeds in a similar fashion as that described for heatup with the following exceptions: We note from Figure 3b that during cooldown the 1/4T location always controls the maximum stress since the thermal gradient produces tensile stresses at the 1/4T location. Thus the steady state pressure is the same as that given in Equation (12). For each cooldown rate, the maximum pressure is evaluated at the 1/4T location from

$$P_{max}(1/4T) = \frac{K_{IR} - K_{It}}{2M_m \left(\frac{r_i^2}{r_o^2 - r_i^2}\right)\left(\frac{r_o^2 + (3/4r_i + 1/4r_o)^2}{(3/4r_i + 1/4r_o)}\right)} \qquad (14)$$

where K_{IR} is obtained from Equation (3) using the material temperature and RT_{NDT} at the 1/4T location. K_{It} is determined from the thermal analysis described in Section D.

It is of interest to note that during cooldown the material temperature will lag the coolant temperature and, therefore, the steady state pressure, which is evaluated at the coolant temperature, will initially yield the lower maximum allowable pressure. When the thermal gradients increase, the stresses do likewise, and, finally, the transient analysis governs the maximum allowable pressure. Hence a point-by-point

comparison must be made between the maximum allowable pressures produced by steady state analyses and transient thermal analysis to determine the minimum of the maximum allowable pressures.

3. Core Operation

At all times that the reactor core is critical, the temperature must be higher than that required for inservice hydrostatic testing, and in addition, the pressure-temperature relationship shall provide at least a 40 °F margin over that required for heatup and cooldown operations. Thus the pressure-temperature limit curves for core operation may be constructed directly from the inservice leak and hydrostatic test and heatup analysis results.

D. Thermal Stress Analysis

The equivalent linear stress due to thermal gradients is obtained from a detailed thermal analysis of the vessel. The temperature distribution in the vessel wall is governed by the partial differential equation

$$\rho c T_t - K\left[(1/r)\,T_r + T_{rr}\right] = 0 \qquad (15)$$

subject to initial condition

$$T(r, 0) = T_o \ , \qquad (16)$$

and boundary conditions

$$-KT_r(r_i, t) = h\left[T_c(t) - T(r_i, t)\right] , \qquad (17)$$

and

$$T_r(r_o, t) = 0 \tag{18}$$

where

$$T_c = T_o + Rt. \tag{19}$$

ρ is the material density, c the material specific heat, K the heat conductivity of the material, h the heat transfer coefficient between the water coolant and vessel material, R the heating rate, T_o the initial coolant temperature, $T(r,t)$ the temperature distribution in the vessel, r the spatial coordinate, and t the temporal coordinate.

A finite difference solution procedure is employed to solve for the radial temperature distribution at various time steps along the heatup or cooldown cycle. The finite difference equations for N radial points, at distance Δr apart, across the vessel are:

for $1 < n < N$

$$T_n^{t+\Delta t} = \left[1 - \frac{\Delta t K}{\rho c (\Delta r)^2}\left(2 + \frac{\Delta r}{r_n}\right)\right] T_n^t + \frac{\Delta t K}{\rho c (\Delta r)^2}\left[\left(1 + \frac{\Delta r}{r_n}\right) T_{n+1}^t + T_{n-1}^t\right], \tag{20}$$

for $n = 1$

$$T_1^{t+\Delta t} = \left[1 - \frac{\Delta t K}{\rho c (\Delta r)^2}\left(1 + \frac{\Delta r}{r_1}\right) - \frac{\Delta t h}{\rho c (\Delta r)}\right] T_1^t + \frac{\Delta t K}{\rho c (\Delta r)^2}\left[\left(1 + \frac{\Delta r}{r_1}\right) T_2^t + \frac{\Delta r h}{K} T_c^t\right], \tag{21}$$

and for n = N

$$T_N^{t+\Delta t} = \left[1 - \frac{\Delta t K}{\rho c (\Delta r)^2}\right] T_N^t + \frac{K \Delta t}{\rho c (\Delta r)^2} T_{N-1}^t \quad . \tag{22}$$

For stability in the finite difference operation, we must choose Δt for a given Δr such that both

$$\frac{\Delta t K}{\rho c (\Delta r)^2} \left(2 + \frac{\Delta r}{r_1}\right) \leq 1 \tag{23}$$

and

$$\frac{\Delta t K}{\rho c (\Delta r)^2} \left(1 + \frac{\Delta r}{r_1}\right) + \frac{\Delta t h}{\rho c (\Delta r)} \leq 1 \tag{24}$$

are satisfied. These conditions assure us that heat will not flow in the direction of increasing temperature, which, of course, would violate the second law of thermodynamics.

Since a large variation in coolant temperature is considered, the dependence of $(K/\rho c)$, K, and h on temperature is included in the analysis by treating these as constants only during every 5°F increment in coolant temperature and then updating their values for the next 5°F increment. The dependence of $(K/\rho c)$ called the thermal diffusivity and K, the thermal conductivity, can be determined from the ASME Boiler and Pressure Vessel Code, Section III, Appendix I - Stress Tables. A linear regression analysis of the tabular values resulted in the following expressions:

$$K(T) = 38.211 - 0.01673 * T \text{ (BTU/HR-FT-°F)} \tag{25}$$

and

$$k(T) = (K/\rho c) = 0.6942 - 0.000432 * T \ (FT^2/HR) \tag{26}$$

where T is in degrees Fahrenheit.

The heat transfer coefficient is calculated based on forced convection under turbulent flow conditions. The variables involved are the mean velocity of the fluid coolant, the equivalent (hydraulic) diameter of the coolant channel, and the density, heat capacity, viscosity, and thermal conductivity of the coolant. For water coolant, allowance for the variations in physical properties with temperature may be made by writing*

$$h(T) = 170(1 + 10^{-2} * T - 10^{-5} * T^2) \ v^{0.8}/D^{0.2} \tag{27}$$

where v is in ft/sec, D in inches, the temperature is in °F, and h is in Btu/hr-ft^2-°F. The values for the heat-transfer coefficient given by this relationship are in good agreement with those obtained from the Dittus-Boelter equation for temperatures up to 600°F. The mean velocity of the coolant, v, is generally given in terms of the effective coolant flow rate Q (Lbm/hr) and effective flow area A (ft^2). Given the relationship

$$\rho(T) = 62.93 - 0.48 \times 10^{-2} * T - 0.46 \times 10^{-4} * T^2 \tag{28}$$

for the density of water as a function of temperature, the mean velocity of the coolant is obtained from

$$v = Q/(3600 * \rho(T) * A) \ . \tag{29}$$

---

* Glasstone, S., Principles of Nuclear Reactor Engineering, D. Van Nostrand Co., Inc., New Jersey, pp. 667-668, 1960.

The thermal stress distribution is calculated from

$$\sigma_T(r,t) = \frac{\alpha E}{1-\nu}\left[\frac{1}{r^2}\int_{r_i}^{r} T(r,t)\,r\,dr - T(r,t) + \frac{1}{r^2}\left(\frac{r^2+r_i^2}{r_o^2-r_i^2}\right)\int_{r_i}^{r_o} T(r,t)\,r\,dr\right] \quad (30)$$

where α is the coefficient of thermal expansion (in/in °F), E is Young's modulus, and ν is Poisson's ratio. This expression can be obtained from Theory of Elasticity by Timoshenko and Goodier, pp. 408-409, when imposing a zero radial stress condition at the cylinder inner and outer radius. Poisson's ratio is taken to be constant at a value of 0.3 while α and E are evaluated as a function of the average temperature across the vessel

$$T_{avg} = \frac{2}{(r_o^2 - r_i^2)}\int_{r_i}^{r_o} T(r)\,r\,dr \quad . \quad (31)$$

The dependence of the coefficient of thermal expansion on temperature is taken to be

$$\alpha(T) = 5.76 \times 10^{-6} + 4.4 \times 10^{-9} * T \quad (32)$$

and the dependence of Young's modulus on temperature is taken to be

$$E(T) = 27.9142 + 2.5782 \times 10^{-4} * T - 6.5723 \times 10^{-6} * T^2 \quad (33)$$

as obtained from regression analysis of tabular values given in Section III, Appendix I of the ASME Boiler and Pressure Vessel Code.

The resulting stress distribution given by Equation (30) is not linear; however, an equivalent linear stress distribution is determined from the resulting moment. The moment produced by the nonlinear

stress distribution is given by

$$M(t) = b\int_{r_i}^{r_o} \sigma_T(r,t)\, r\, dr \tag{34}$$

where b is a unit depth of the vessel. Here we note that the moment is a function of time, i.e., coolant temperature via $T_c = To + Rt$. For a linear stress distribution we have that

$$\sigma_{max} = \frac{Mc}{I} \tag{35}$$

where σ_{max} is the maximum outer fiber stress, c the distance from the neutral axis, taken to be $(r_o - r_i)/2$, and I the section area moment of inertia which is given by

$$I = \frac{bh^3}{12} = \frac{b(r_o - r_i)^3}{12} \quad . \tag{36}$$

Combining these expressions results in the equivalent linear stress due to thermal gradients

$$\sigma_{max} = \sigma_{bt} = \frac{6}{(r_o - r_i)^2}\int_{r_i}^{r_o} \sigma_T(r,t)\, r\, dr \tag{37}$$

The thermal stress intensity factor K_{It} is then defined as

$$K_{It} = M_b\, \sigma_{bt} \tag{38}$$

where M_b is determined from the curves given in Figure 1 wherein $M_b = 2/3\, M_m$. It is of interest to note that a sign change occurs in the stress calculations during a cooldown analysis since the thermal gradients

produce compressive stresses at the vessel outer radius. This sign change must then be reflected in the K_{It} calculation for the cooldown analysis.

Normalized temperature and thermal stress distributions during a typical reactor heatup are given in Figure 4. The radial temperature is shown normalized with respect to the average temperature, T_{avg}, by

$$T = \frac{T - T_{avg}}{(T - T_{avg})_{max}} \quad . \tag{39}$$

The thermal stress and equivalent linearized stress, as calculated by Equations (30) and (37), are normalized with respect to the maximum thermal stress. Here we note that the actual thermal stress at the 3/4T location is considerably less than the maximum equivalent linear stress which yields additional safety margins during the heatup cycle. Similar temperature and thermal stress distributions are developed during cooldown. The trends are nearly identical as those shown in Figure 4 when the inner and outer vessel locations are reversed with the 1/4T location becoming the critical point.

E. Example Calculations

The following example is based on a reactor vessel with the following characteristics:

Inner Radius	=	82.00 in.	(r_i)
Outer Radius	=	90.00 in.	(r_o)
Operating Pressure	=	2250 psig	(P_o)

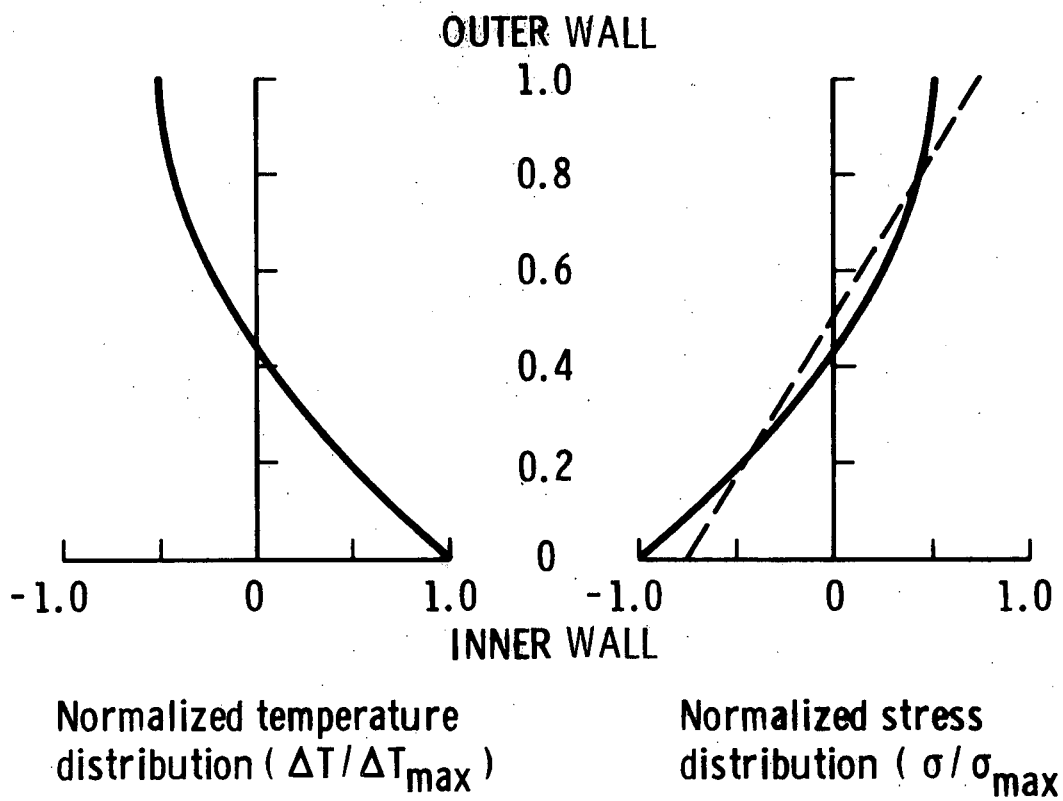

Figure 4. Typical Normalized Temperature and Stress Distribution During Heatup

Initial Temperature	=	70°F	(T_o)
Final Temperature	=	550°F	(T_f)
Effective Coolant Flow Rate	=	100×10^6 Lbm/hr	(Q)
Effective Flow Area	=	20.00 ft^2	(A)
Effective Hydraulic Diameter	=	10.00 in.	(D)
RT_{NDT} (1/4T)	=	200°F	
RT_{NDT} (3/4T)	=	140°F	

In the thermal stress analysis 21 radial points were used in the finite difference scheme. Going from 70°F to the final temperature of 550°F, approximately 12,000 time (temperature via T = To + Rt) steps were required in the thermal analysis for the 100°F/hr heatup rate. The results of the computation are shown in Figures 5 through 9.

Figure 5 gives the reference stress intensity factor, K_{IR}, as a function of temperature indexed to RT_{NDT} (1/4T). For the steady state analysis, K_{IR} is converted directly to allowable pressure via Equation 12.

During the heatup and cooldown thermal analyses the material temperature at the 1/4T and 3/4T and thermal stress intensity factors K_{It} are required to compute allowable pressure via Equations (13) and (14). The material temperatures versus coolant temperature during the 100°F/hr heatup and cooldown analyses are given in Figure 6. These temperatures allow computation of the corresponding reference stress intensity factors, K_{IR} (3/4T) and K_{IR} (1/4T). Figure 7 gives the corresponding thermal stress intensity factor at the 3/4T and 1/4T locations as a function of coolant temperature.

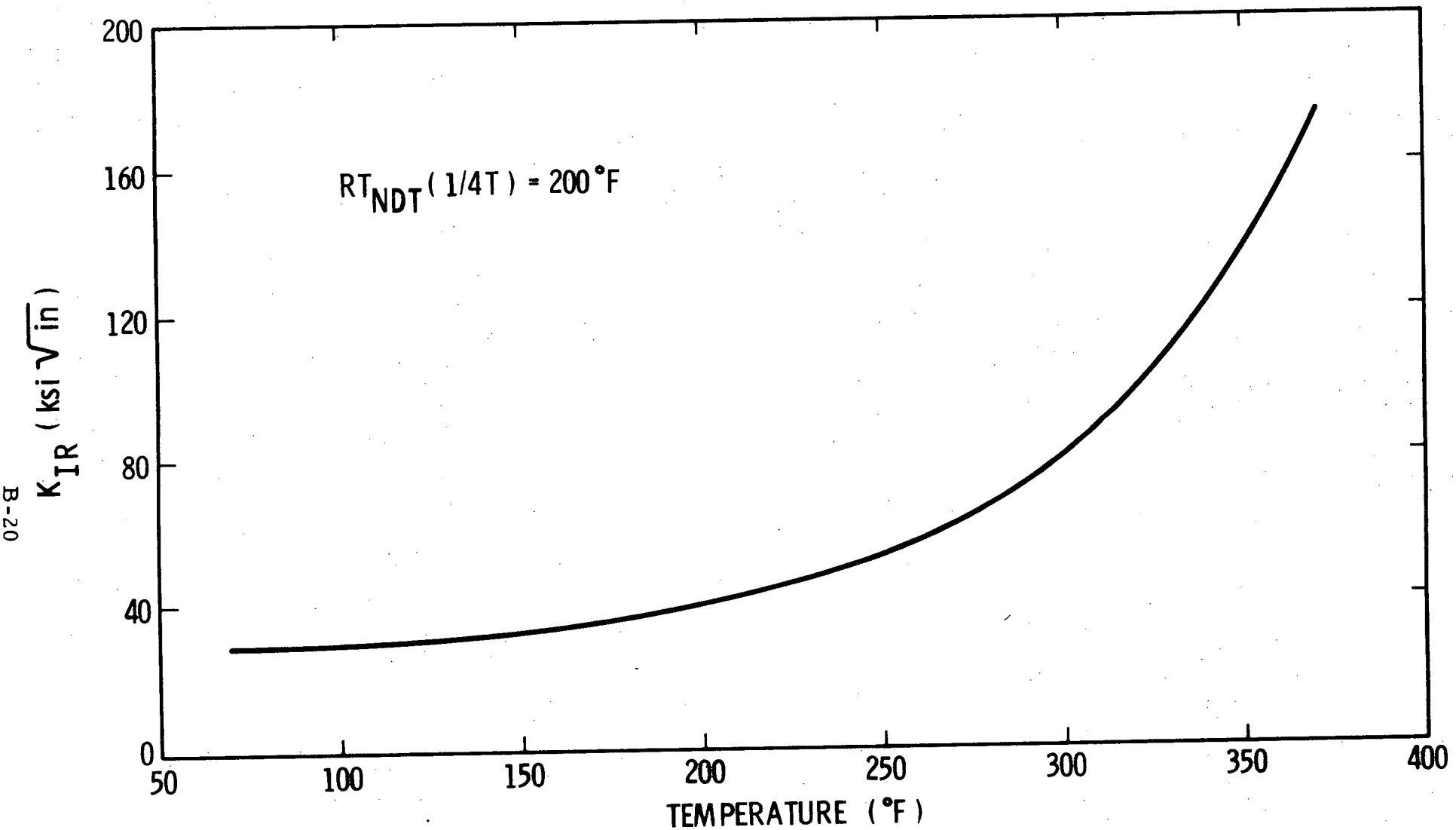

Figure 5. Reference Stress Intensity Factor as a Function of Temperature Indexed to RT_{NDT} (1/4T)

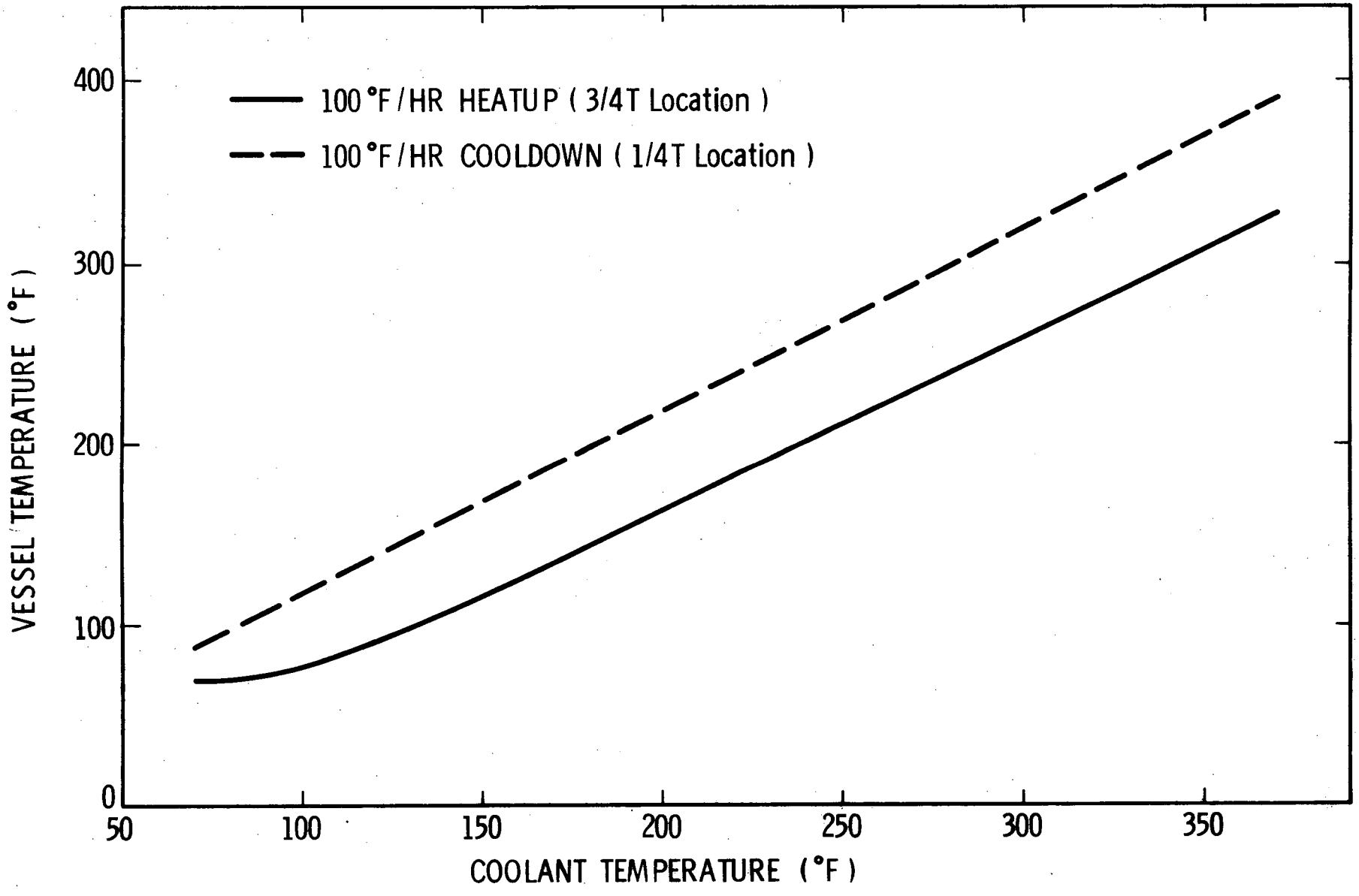

Figure 6. Vessel Temperature at 1/4T and 3/4T Locations as a Function of Coolant Temperature

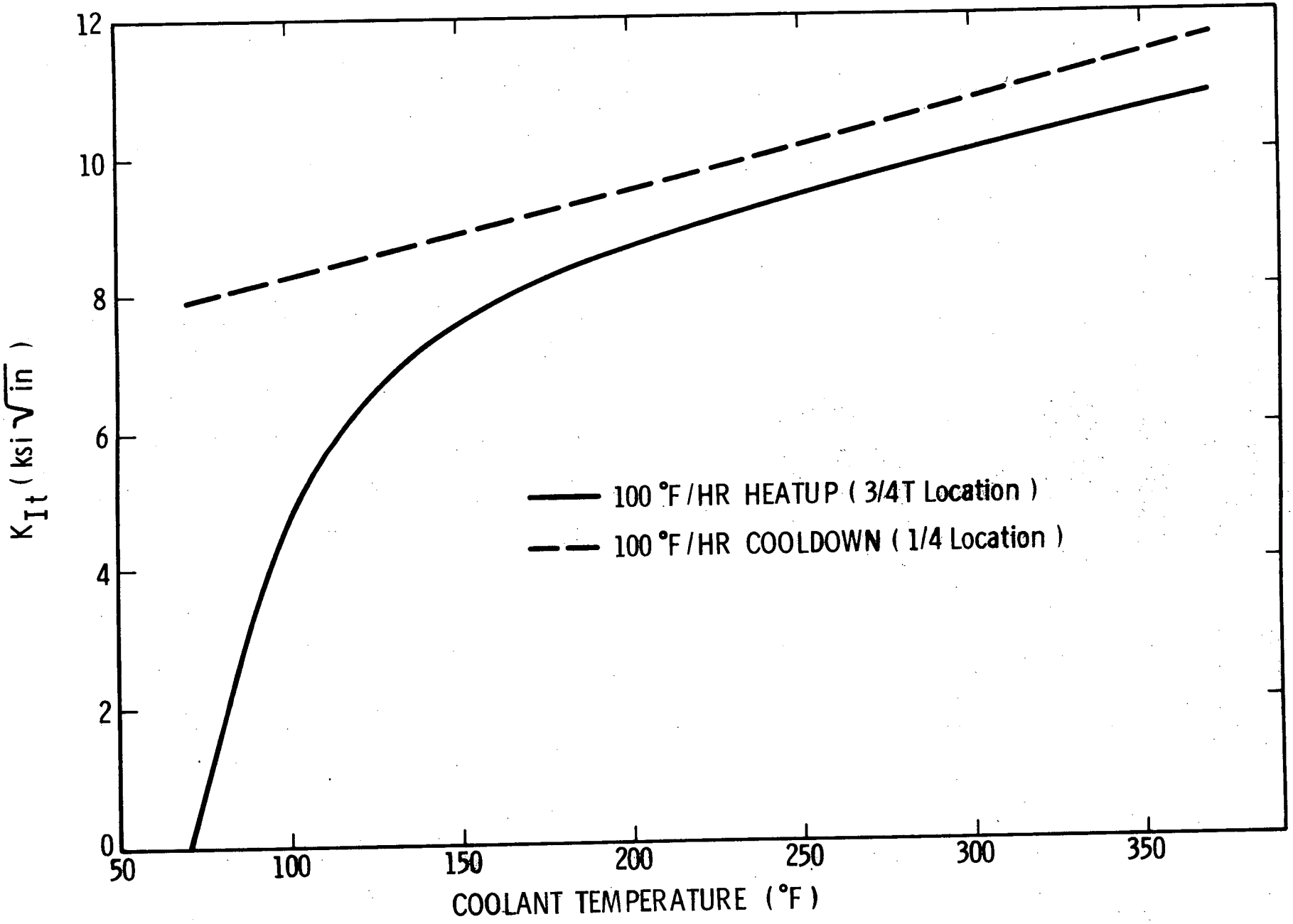

Figure 7. Thermal Stress Intensity Factor at 3/4T and 1/4T Locations as a Function of Coolant Temperature

Figures 8 and 9 demonstrate the construction of the allowable composite pressure and temperature curves for the 100°F/hr heatup and cooldown rates. The composite curves represent the lower bound of the thermal and steady state curves with the addition of margins of +10°F and -60 psig for possible instrumentation error. Figure 8 also shows the leak test limit, corrected for instrument error, as obtained from Equation (9). The limit points are at the operating pressure 2250 psig and at 2475 psig which corresponds to 1.1 times the operating pressure. The criticality limit is also shown in Figure 8 and is constructed by providing for a 40°F margin over that required for heatup and cooldown and by requiring that the minimum temperature be greater than that required by the leak test limit.

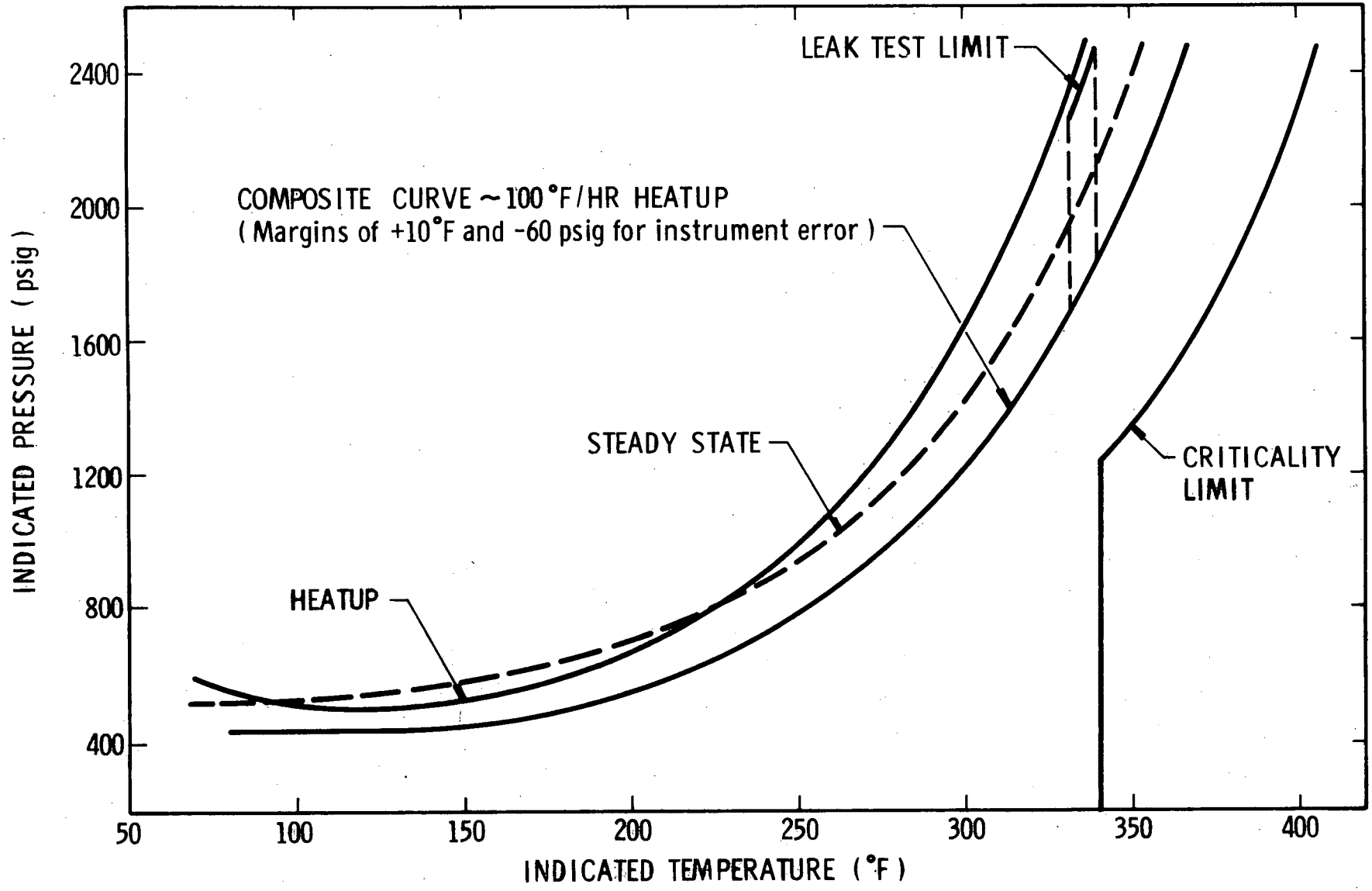

Figure 8. Pressure-Temperature Curves for 100°F/Hr Heatup

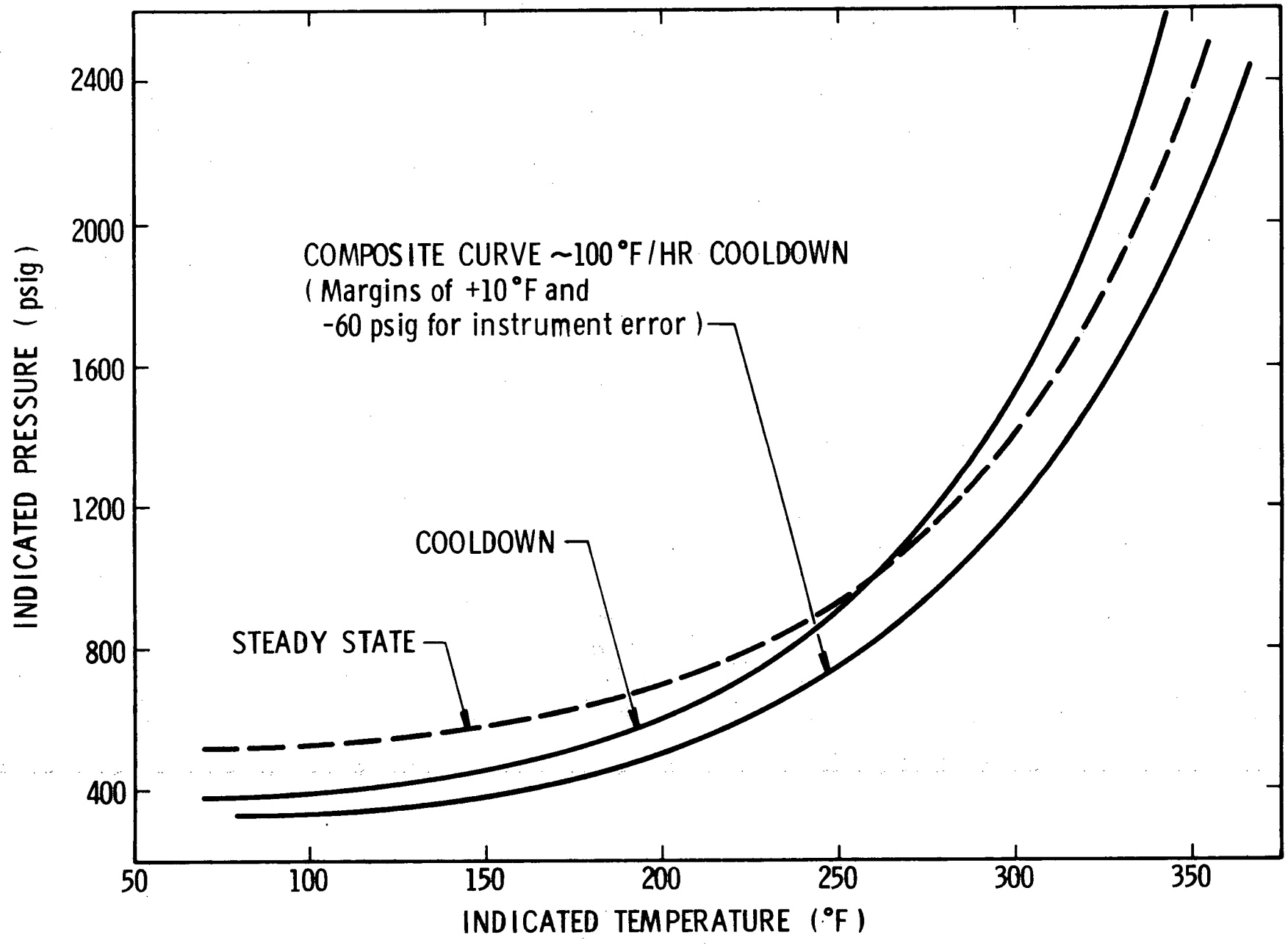

Figure 9. Pressure-Temperature Curves for 100°F/Hr Cooldown